NAVAL AIR WARFARE CENTER AIRCRAFT DIVISION
PATUXENT RIVER, MARYLAND

TECHNICAL REPORT

REPORT NO: NAWCADPAX/TR-2006/140

TESTING OF 7050-T7451 ALUMINUM STRAIN-LIFE COUPONS FOR A PROBABILISTIC STRAIN-LIFE CURVE

by

Mr. David T. Rusk, P.E.
Mr. Robert E. Taylor
Dr. Paul C. Hoffman, P.E.

2 November 2006

DEPARTMENT OF THE NAVY
NAVAL AIR WARFARE CENTER AIRCRAFT DIVISION
PATUXENT RIVER, MARYLAND

NAWCADPAX/TR-2006/140
2 November 2006

TESTING OF 7050-T7451 ALUMINUM STRAIN-LIFE COUPONS FOR A PROBABILISTIC STRAIN-LIFE CURVE

by

Mr. David T. Rusk, P.E.
Mr. Robert E. Taylor
Dr. Paul C. Hoffman, P.E.

RELEASED BY:

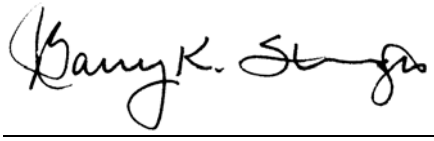

2 Nov 2006
BARRY STURGIS / AIR-4.3.3 / DATE
Head, Structures Division
Naval Air Warfare Center Aircraft Division

REPORT DOCUMENTATION PAGE

Form Approved
OMB No. 0704-0188

1. REPORT DATE	2. REPORT TYPE	3. DATES COVERED
2 November 2006	Technical Report	1 October 2000 – 30 September 2004

4. TITLE AND SUBTITLE

Testing of 7050-T7451 Aluminum Strain-Life Coupons for a Probabilistic Strain-Life Curve

5a. CONTRACT NUMBER

5b. GRANT NUMBER

5c. PROGRAM ELEMENT NUMBER

6. AUTHOR(S)

Mr. David T. Rusk, P.E.
Mr. Robert E. Taylor
Dr. Paul C. Hoffman, P.E.

5d. PROJECT NUMBER

5e. TASK NUMBER

5f. WORK UNIT NUMBER

7. PERFORMING ORGANIZATION NAME(S) AND ADDRESS(ES)

Structures Division, Code 4.3.3
Bldg. 2187, Suite 2340A
Naval Air Systems Command
48110 Shaw Road, Unit #5
Patuxent River, MD 20670-1906

8. PERFORMING ORGANIZATION REPORT NUMBER

NAWCADPAX/TR-2006/140

9. SPONSORING/MONITORING AGENCY NAME(S) AND ADDRESS(ES)

NAVSTO, Code 4.0X
Bldg. 2109, N122
Naval Air Systems Command
48150 Shaw Road Unit 5
Patuxent River, Maryland 20670-1907

10. SPONSOR/MONITOR'S ACRONYM(S)

11. SPONSOR/MONITOR'S REPORT NUMBER(S)

12. DISTRIBUTION/AVAILABILITY STATEMENT

Approved for public release; distribution is unlimited.

13. SUPPLEMENTARY NOTES

14. ABSTRACT

Fleet life tracking is an integral part of NAVAIR's approach to ensuring the airworthiness and operational readiness of U.S. Naval Aviation assets. Historically, life limits for Naval airframe components have been derived by deterministic analyses of stress-life or strain-life fatigue models. To improve fatigue life prediction capabilities for airframe structures, NAVAIR has begun development of a Probabilistic Strain-Life model. As a first step in the development of the Probabilistic Strain-Life method, an extensive testing program was initiated to characterize the scatter in standard ASTM strain-life test coupons for 7050-T7451 aircraft aluminum. Two different coupon geometries are described in the relevant standards: an axially loaded, uniform gage section test coupon and an axially loaded, hourglass gage section coupon. Both coupon types were investigated to determine the differences in fatigue life characteristics between the two. Two different test laboratories were also utilized for testing, to obtain a measure of interlaboratory variation in fatigue results. This investigation shows that the choice of coupon geometry, test procedures, and the test laboratory all have an effect on the statistics of the strain-life test results. From these tests, a probabilistic strain-life curve can be developed to characterize the scatter in material fatigue resistance.

15. SUBJECT TERMS

Fleet Life Tracking Strain-Life Testing Strain-Life Curve Probabilistic Strain-Life Fatigue Testing

16. SECURITY CLASSIFICATION OF:			17. LIMITATION OF ABSTRACT	18. NUMBER OF PAGES	19a. NAME OF RESPONSIBLE PERSON
a. REPORT	b. ABSTRACT	c. THIS PAGE			19b. TELEPHONE NUMBER (include area code)
Unclassified	Unclassified	Unclassified	SAR	70	David Rusk (301) 342-9428

Standard Form 298 (Rev. 8-98)
Prescribed by ANSI Std. Z39-18

SUMMARY

Fleet life tracking is an integral part of NAVAIR's approach to ensuring the airworthiness and operational readiness of U.S. Naval Aviation assets. Historically, life limits for Naval airframe components have been derived by deterministic analyses of stress-life or strain-life fatigue models, with knock-down factors often used to provide the necessary conservatism, and to ensure that the prediction matches known component failure lives. To improve fatigue life prediction capabilities for airframe structures, NAVAIR has begun development of a Probabilistic Strain-Life model, which should reduce the need for conservative knock-down factors in the existing deterministic approach, and also provide measures of reliability and confidence for future airframe life predictions. As a first step in the development of the Probabilistic Strain-Life method, an extensive testing program was initiated to characterize the scatter in standard ASTM strain-life test coupons for 7050-T7451 aircraft aluminum. Two different coupon geometries are described in the relevant standards: an axially loaded, uniform gage section test coupon and an axially loaded, hourglass gage section coupon. Both coupon types were investigated to determine the differences in fatigue life characteristics between the two. Two different test laboratories were also utilized for testing, to obtain a measure of interlaboratory variation in fatigue results.

This investigation shows that the choice of coupon geometry, test procedures, and the test laboratory all have an effect on the statistics of the strain-life test results. The most important variable in determining the fatigue life scatter of strain-controlled tests is in the choice of coupon geometry. The use of an hourglass coupon geometry also requires attention to the microstructure of the base material used to fabricate the coupons. If a preferred grain orientation exists in the material, strain-life test procedures must be utilized that will control the diametral extensometer location with respect to the grain direction. For strain-controlled tests, uniform gage coupon lives have less mean, and less scatter than hourglass coupons tested with a random grain orientation, and less mean, but more scatter compared to hourglass coupons tested with the grain orientation controlled. In the load-controlled tests results, there was no significant difference between the two coupon types in the finite life region, but the endurance limit for the uniform gage coupon was slightly lower. For the sample sizes tested, there was also no significant difference in the strain-life or load-life results generated by the two test labs, except that the endurance limits were somewhat different. In several cases in this investigation, sample sizes were insufficient to clearly distinguish differences in population variances. Further statistical analysis of the test results is necessary to better define the test sample sizes needed to fully capture the variation in material fatigue resistance, especially with regard to the fitting of probabilistic strain-life curves.

Contents

List of Tables

List of Figures

ACKNOWLEDGEMENTS

The authors wish to thank Mr. Moise Devillier of the NAVAIR Science and Technology Office (NAVSTO) Code 4.0X, for supporting the probabilistic strain life work described in this report.

INTRODUCTION

Fleet life tracking is an integral part of NAVAIR's approach to ensuring the airworthiness and operational readiness of U.S. Naval Aviation assets. The ability to predict the fatigue life of an airframe component is essential to set realistic service life limits for repair and replacement. Historically, life limits for Naval airframe components have been derived by deterministic analyses of stress-life or strain-life fatigue models, correlated with results from a single full-scale fatigue test. The fatigue models developed for airframe life tracking are primarily based on the strain-life approach, which has the advantage over stress-life approaches of being able to treat local plastic yielding in notched structures, as well as the effect of periodic overloads on fatigue life (reference 1). Much of the developmental and verification efforts carried out on the strain-life method focused on validating the method's ability to deterministically predict the crack initiation life of a notched component, with a sufficient degree of conservatism to warrant engineering confidence in the prediction (references 2 and 3). Knock-down factors are often used to provide the necessary conservatism, and to ensure that the prediction matches known component failure lives.

To improve fatigue life prediction capabilities for airframe structures, NAVAIR has begun development of a Probabilistic Strain-Life model, which should reduce the need for conservative knock-down factors in the existing deterministic approach, and also provide measures of reliability and confidence for future airframe life predictions. As a first step in the development of the Probabilistic Strain-Life method, an extensive testing program was initiated to characterize the scatter in standard ASTM strain-life test coupons for 7050-T7451 aircraft aluminum. Two different coupon geometries are described in the relevant standards: an axially loaded, uniform gage section test coupon and an axially loaded, hourglass gage section coupon. Both coupon types were investigated to determine their differences in fatigue life characteristics. Two different test laboratories were also utilized for testing, to obtain a measure of interlaboratory variation in fatigue results. This report describes the methods utilized to conduct testing, and discusses the effect of different hourglass coupon test procedures on the results. An analysis of test results is provided, with a complete listing of raw results data from all fatigue tests in appendix A. From these results, a probabilistic strain-life curve can be developed to characterize the scatter in material fatigue resistance.

METHODS

TEST COUPONS

ASTM E606 is the standard that governs the fabrication and testing of strain-life coupons (reference 4). The standard identifies two different coupon geometries: an axially loaded, uniform gage section test coupon and an axially loaded, hourglass gage section coupon. To examine coupon geometry effects on test results, both uniform gage and hourglass coupons were fabricated and tested. All hourglass test coupons were cut from a single rolled plate of 7050-T7451 aluminum (Plate 1) conforming to AMS-4050 standards. The plate dimensions were 0.50 in. x 48.5 in. x 144.5 in. Chemical composition of the plate is shown in table 1. Hourglass coupons have a 1.5 in. radius of curvature, a 0.25 in. nominal diameter, and a 0.485 in. grip diameter. These coupons are identified as the HG1 configuration in the test matrix. Three different uniform gage coupon geometries were manufactured for the test program. The first is identified as the UG1 configuration, and has a 0.25 in. nominal diameter, a 1.0 in. long reduced cross-section, a 0.50 in. transition radius, and a 0.485 in. grip diameter. The second is identified as the UG2 configuration, and has a 0.375 in. nominal diameter, a 1.0 in. long reduced cross-section, a 0.50 in. transition radius, and a 0.485 in. grip diameter. This coupon has an increased test section diameter to alleviate compressive buckling problems encountered with UG1 coupons at strain amplitudes above 1.5%. Both UG1 and UG2 coupons were cut from Plate 1. UG3 coupons have a 0.25 in. nominal diameter, a 0.75 in. long reduced cross-section, a 1.0 in. transition radius, and a 0.50 in. grip diameter. These coupons were cut from a rolled 7050-T7451 plate of dimensions 0.625 in. x 20.25 in. x 94.625 in. (Plate 2). Chemical composition of this plate is shown in table 2. Individual coupon dimensions are also shown in figure 1. All of the test coupons were manufactured by Metcut Research, Inc., and were cut with their axial loading direction parallel to the rolling direction of their respective plates, with an 8 μin. surface finish specified.

Table 1: Chemical Composition of HG1, UG1, and UG2 Test Coupons (% Weight)

CR	CU	FE	MG	MN	SI	TI	ZN	ZR	Other
0.01	2.2	0.07	2.0	0.02	0.03	0.02	6.4	0.11	0.15

Table 2: Chemical Composition of UG3 Test Coupons (% Weight)

CR	CU	FE	MG	MN	SI	TI	ZN	ZR	Other
<0.01	2.2	0.08	2.0	<0.01	0.4	0.03	6.3	0.11	0.15

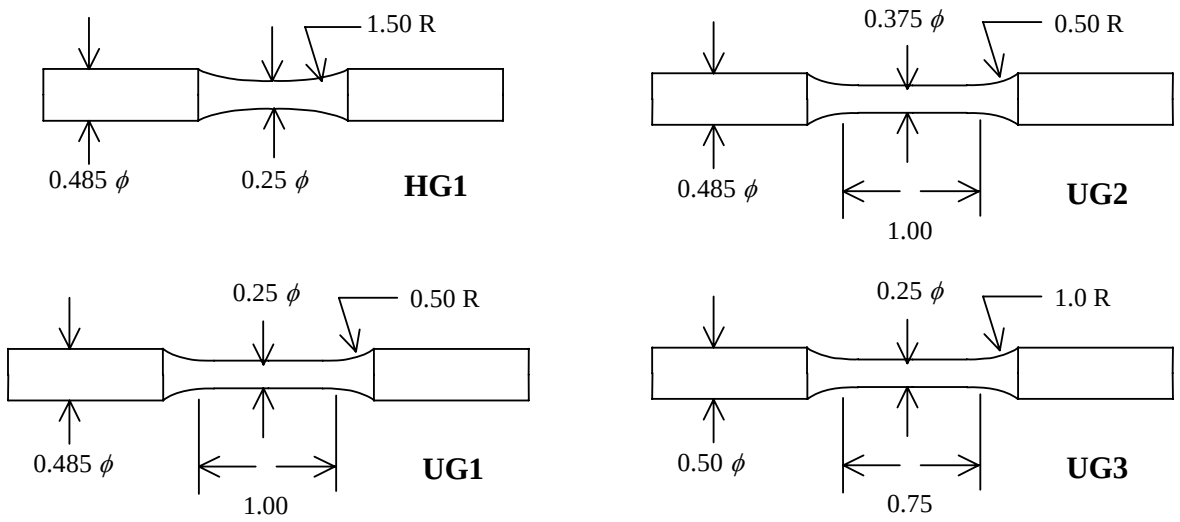

Figure 1: Strain-Life Test Coupon Geometries

TENSILE AND INCREMENTAL STEP PROCEDURES

Tensile tests were performed by the NAVAIR Metallic Materials Test Laboratory (Code 4.3.4.2) on 10 UG1 coupons to obtain static tensile strength properties and monotonic stress-strain curves. ASTM E8 is the standard that governs tensile test procedures (reference 5). Since it was desired to obtain tensile properties and full stress-strain curves from the same coupon tests, some modifications to the test procedures were made. ASTM E646 is the standard that governs testing to obtain strain-hardening exponents for ductile materials (reference 6). It specifies that the speed of testing shall be between 0.05 and 0.50 in./in./min. However, when testing for yield properties, E8 specifies that the rate of stress application shall be between 10,000 and 100,000 psi/min., which for aluminum translates to a strain rate of between 0.001 and 0.01 in./in./min. To satisfy both criteria, the 7050 tensile coupons were first strained at a rate of approximately 0.005 in./in./min. to slightly beyond the 0.2% strain offset yield point, after which they were strained at a rate of approximately 0.2 in./in./min. until final failure. The strain rate transition point for most tests was at 1.1% in./in. strain. Load, stroke, and strain values were digitally recorded for all of the tests, at a sampling rate that varied between 1 and 10 Hz. The jump in strain rate beyond the yield point creates a small spike in the recorded stress-strain data, which was subsequently smoothed out during postprocessing. Elastic modulus values were obtained by regressing the recorded stress-strain data from each test.

Strain-controlled tests were performed by Code 4.3.4.2 on 10 UG2 coupons to obtain cyclic stress-strain curves for the material at room temperature in laboratory air. An incremental step test procedure was used, where the coupon is subjected to repeated blocks of gradually decreasing and increasing strain amplitude (reference 7). The test blocks had an initial maximum peak strain amplitude of 2.0%, with subsequent tensile peaks stepped down in increments of 0.05% strain (figure 2). After the material cyclically stabilizes, the hysteresis loop tips can be connected to yield the cyclic stress-strain curve (figure 3). For the strain profile used, the

material cyclically stabilized by the third incremental step block application. Strain rate for testing was 0.02 in./in./sec. Load and strain data were digitally recorded throughout each test, at a sampling rate of 200 Hz.

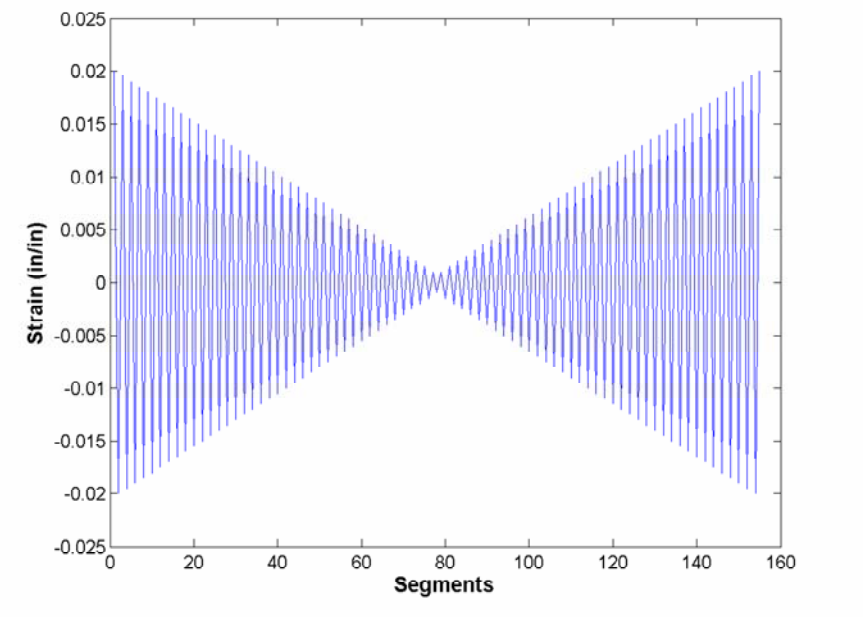

Figure 2: Block of Incremental Step Strain History

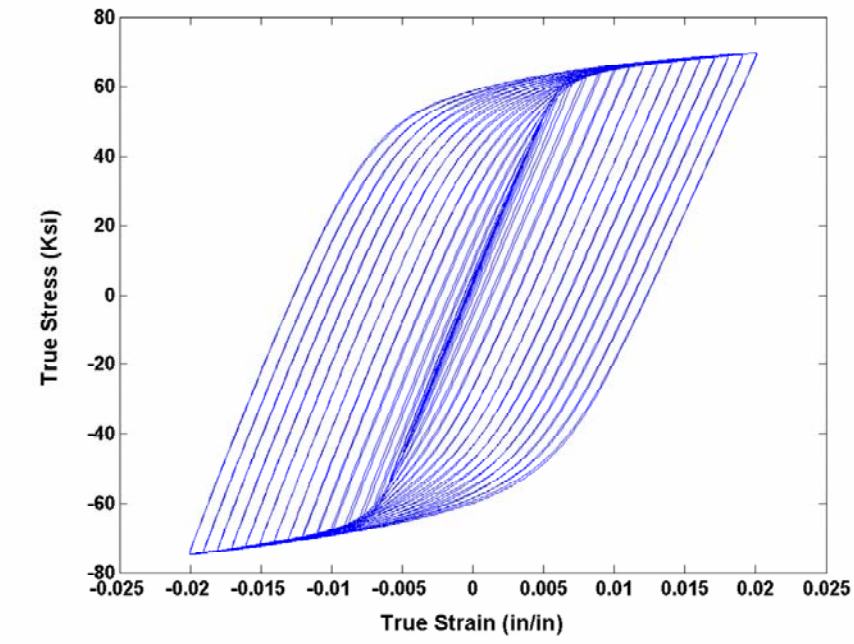

Figure 3: Hysteresis Loop Progression for Block of Incremental Step Test Loading

Since the strain peaks are incrementally decreasing and increasing, it takes one complete pass through the loading block to give complete, fully-reversed hysteresis loops at all of the strain amplitudes tested. Hysteresis half-cycles can be derived from the descending and ascending strain range portions of the loading block, but have slightly different stress ranges, and give different cyclic stress-strain curves (figure 4). This effect was described by Landgraf, et al, as resulting from the cyclic history dependence of some metals (reference 8). For all of the incremental step tests in this study, the final cyclic stress-strain curves were derived by averaging the strain amplitudes from the ascending and descending portions of the loading block.

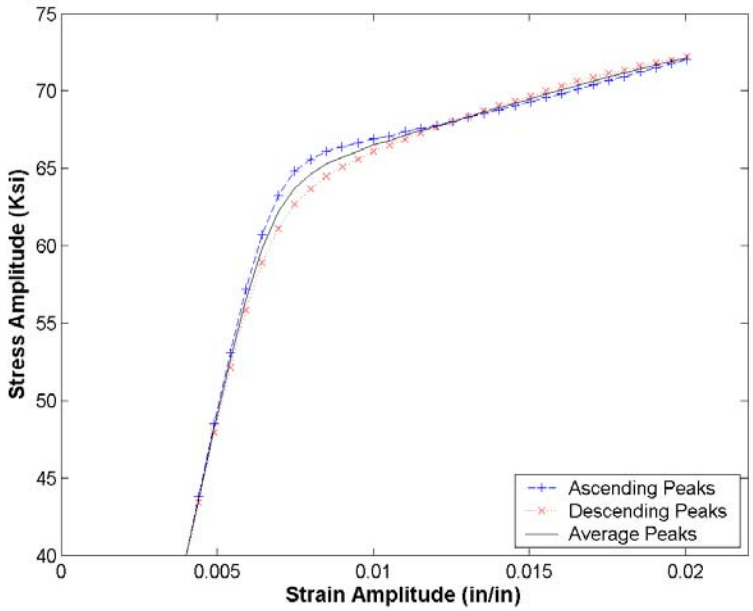

Figure 4: Stabilized Cyclic Stress-Strain Curves from Incremental Step Test Coupon

CONSTANT-AMPLITUDE TEST PROCEDURES

Fully-reversed (R = -1), constant-amplitude, strain-controlled tests were performed using closed-loop servo-controlled hydraulic testing machines in the NAVAIR Metallic Materials Test Laboratory (Code 4.3.4.2), and at Metcut Research, Inc., an independent private test laboratory. All strain-controlled tests were performed in room temperature laboratory air, at an axial strain rate of 2.0% (in./in./sec) with a triangular waveform. Uniform-gage coupons were tested under real-time strain control using an axial extensometer per ASTM E606. Hourglass coupons were tested under axial strain control using a diametral extensometer to measure transverse deflection, which was converted to an axial strain signal by the test frame real-time controller using the conversion equations in ASTM E606, appendix X2. The value for Young's modulus used in the conversion equation was initially set to the average elastic modulus from the tensile test results, and was subsequently rounded off to three significant figures (table 3). The value for elastic Poisson's Ratio is taken from MIL-HDBK-5 (reference 9).

Table 3: Material Coefficients for Conversion of 7050-T7451 Diametral Strain to Axial Strain

Cyclic Elastic Modulus	10,100 Ksi
Poisson's Ratio	0.33

Load-controlled tests on both uniform-gage and hourglass coupons were also performed at fully-reversed strain amplitudes below the proportional limit of the cyclic stress-strain curve. These tests were performed in room temperature laboratory air in accordance with ASTM E466 (reference 10), using a sinusoidal waveform. For strain-controlled tests with strain-amplitude values below 0.008 (m/m), and for all load-controlled tests, the test coupons were subjected to an initial overstrain loading sequence to simulate the effect that periodic overloads would have on damage accumulation in a notched member under variable-amplitude loading (reference 11). Previous research has shown that the exact number and amplitude of applied overstrain cycles does not affect the resulting fatigue life, within the range of life scatter of the overstrained samples (references 12 and 13). Dowling suggests that the total number of overstrain cycles applied should be only a few percent of the total life corresponding to the overstrain amplitude, to avoid causing premature failures from what would effectively be a high-low step test (reference 14). For the tests in this study, the overstrain sequence consisted of 20 cycles of 1.0% (m/m) axial strain, followed by a cyclic ramping down of the strain peaks to zero (figure 5). The test coupons were then run at constant amplitude until failure. The overload cycles were not counted in the cycles-to-failure results for any of these coupons.

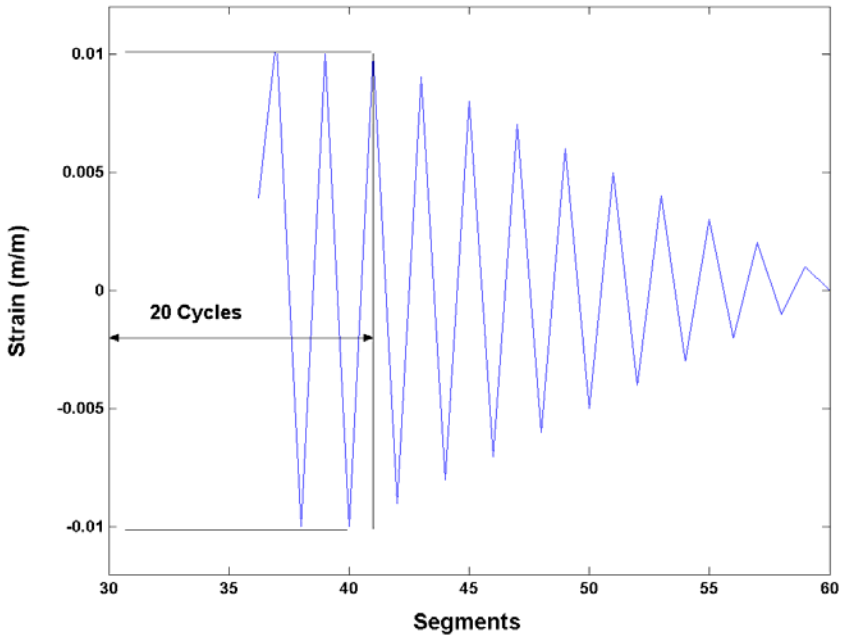

Figure 5: Initial Overstrain Sequence for Low Strain-Amplitude Tests

TEST MATRICES

The overall strain-life testing effort was subdivided into test groups as a function of test lab, coupon type, strain-amplitude values, and testing procedures. A Randomized Complete Block (RCB) test matrix was specified for each group of tests (reference 15), to ensure adequate randomization of test coupons and test sequences for the purpose of statistical data reduction. The details of each test group are listed in table 4.

Table 4: 7050-T7451 Strain-Life Fatigue Test Groups

Test No.	Sample Size	Test Group	Test Lab	Test Type	Coupon Type	Test Strain Amp. (%)
UB-#	40	Uniformity Trial	4.3.4.2	Strain Control	UG1, HG1	0.8, 1.0
UC-#	40	Uniformity Trial	Metcut	Strain Control	UG1, HG1	0.8, 1.0
LP3-#	50	Low Cycle Fatigue Population (LCF Pop.)	4.3.4.2	Strain Control	HG1	1.2, 1.5, 2.0, 3.0, 4.0
LPG1-#	25	LCF Grain-Controlled Pop.	4.3.4.2	Strain Control	HG1	1.2, 1.5, 2.0, 3.0, 4.0
LPG2-#	75	LCF Grain-Controlled Pop.	Metcut	Strain Control	HG1	1.2, 1.5, 2.0, 3.0, 4.0
LPGA1-#	10	LCF Grain-Controlled Pop.	4.3.4.2	Strain Control	HG1	0.8, 1.0
LPGA2-#	29	LCF Grain-Controlled Pop.	Metcut	Strain Control	HG1	0.8, 1.0
LPUG-#	19	LCF Pop.	Metcut	Strain Control	UG3	0.8, 1.0, 1.2, 1.5, 2.0
IP1-#	20	Intermediate Cycle Fatigue Population (ICF Pop.)	4.3.4.2	Strain Control, Initial Overstrain	HG1	0.6, 0.7
IPG1-#	10	ICF Grain-Controlled Pop.	4.3.4.2	Strain Control, Initial Overstrain	HG1	0.6, 0.7
IPG2-#	30	ICF Grain-Controlled Pop.	Metcut	Strain Control, Initial Overstrain	HG1	0.6, 0.7
IPUG-#	9	ICF Pop.	Metcut	Strain Control, Initial Overstrain	UG3	0.6, 0.7
HP1-#	60	High Cycle Fatigue Population (HCF Pop.)	4.3.4.2	Load Control, Initial Overstrain	HG1	0.2, 0.25, 0.3, 0.4, 0.5
HP2-#	60	HCF Pop.	Metcut	Load Control, Initial Overstrain	HG1	0.25, 0.27, 0.3, 0.4, 0.5
HPUG-#	60	HCF Pop.	Metcut	Load Control, Initial Overstrain	UG3	0.25, 0.3, 0.4, 0.5

The LCF Pop. tests were all constant-amplitude, strain-controlled tests at strain amplitudes at or above 1.0%. ICF Pop. tests were those constant-amplitude, strain-controlled tests that had an initial overstrain sequence applied to them. HCF Pop. tests were all constant-amplitude, load-controlled, with an initial overstrain sequence that was strain-controlled. Some hourglass coupons were tested with their microstructure grain orientations controlled with respect to the placement of the diametral extensometer (see DISCUSSION section), while those in groups with no grain control identified were tested with the grain randomly oriented with respect to the diametral extensometer.

FAILURE CRITERIA

For most strain-controlled tests, long crack growth can take up a significant portion of the total life of the coupon. Since it is desired that the fatigue test results represent the life to a short crack size, most of this crack growth must be subtracted out of the total life for each coupon. Failure progression in a strain-controlled test can be tracked by examining the peak load history over the duration of the test. As cracks grow through the coupon cross-section, the residual load capability of the coupon decreases for a constant peak strain value, until final fracture is reached (figure 6).

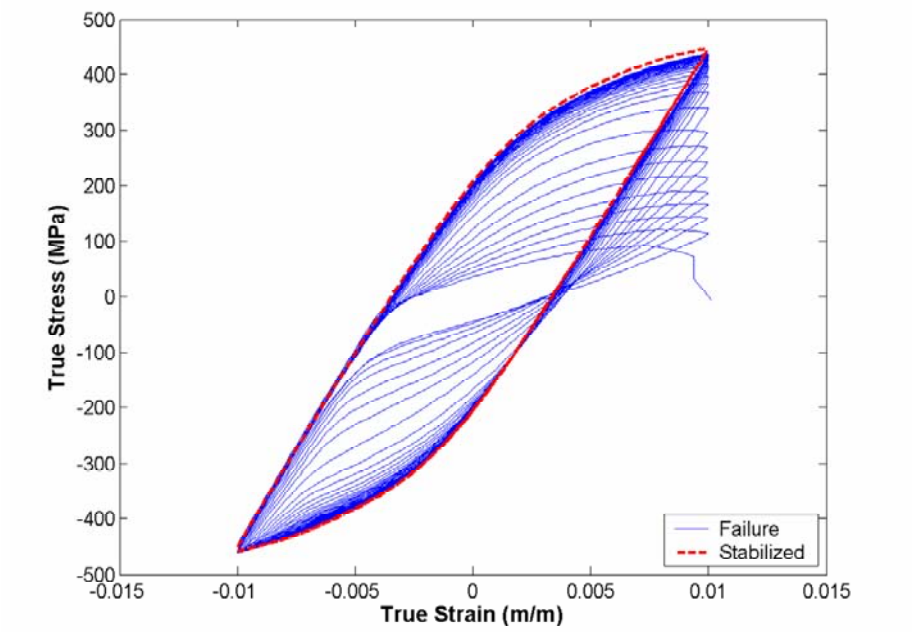

Figure 6: Hysteresis Loop Failure Progression for Strain-Controlled Fatigue Test

By recording the load-strain values throughout the test, a failure criteria based on a percentage of peak load drop from the cyclically stabilized peak load value can be applied to subtract crack growth cycles from the total cycles to failure for each strain-controlled test (reference 16). To enable the use of a load drop percentage failure criteria, all strain-controlled tests performed for this investigation had load-strain values digitally recorded throughout each test, at a data

sampling rate of 100 Hz. The correlation of peak load drop percentages to specific crack depths on the test coupons is currently unknown, so a range of peak load drop percentages was used in the data reduction process to give an indication of how the peak load changes as a function of coupon life. The life to load drop percentages of 2%, 5%, 10%, 15%, 20%, 25%, and 50% were calculated for each coupon. The cyclically stabilized peak load used to reference peak load drop percentages was an average value of three hysteresis loop peaks extracted from the results file at approximately half the total life of the coupon. All coupons tested at a specific strain amplitude used stabilized loop peaks extracted at the same number of cycles, to enable direct comparison of results from coupon to coupon. For load-controlled tests with long lives, only a small percentage of the total life is spent propagating a large crack. For these tests, the total life is assumed to be the life to a short crack size, and no correction for crack growth is made. Dowling has previously investigated these effects for both unnotched and notched tests (reference 17).

TEST RESULTS PRESENTATION

Because of the volume of results generated from this testing effort, a Microsoft Access Database was created to archive the test results for future reference. Use of a relational database allows for fast compilation of result tables for any combination of test parameters in the database. An example of the data stored in the database, and the format used to present the information is shown in figure 7. The information contained in the database was chosen based on the recommendations of ASTM E468 (reference 18) and SAE Surface Vehicle Standard J2409 (reference 19), where applicable.

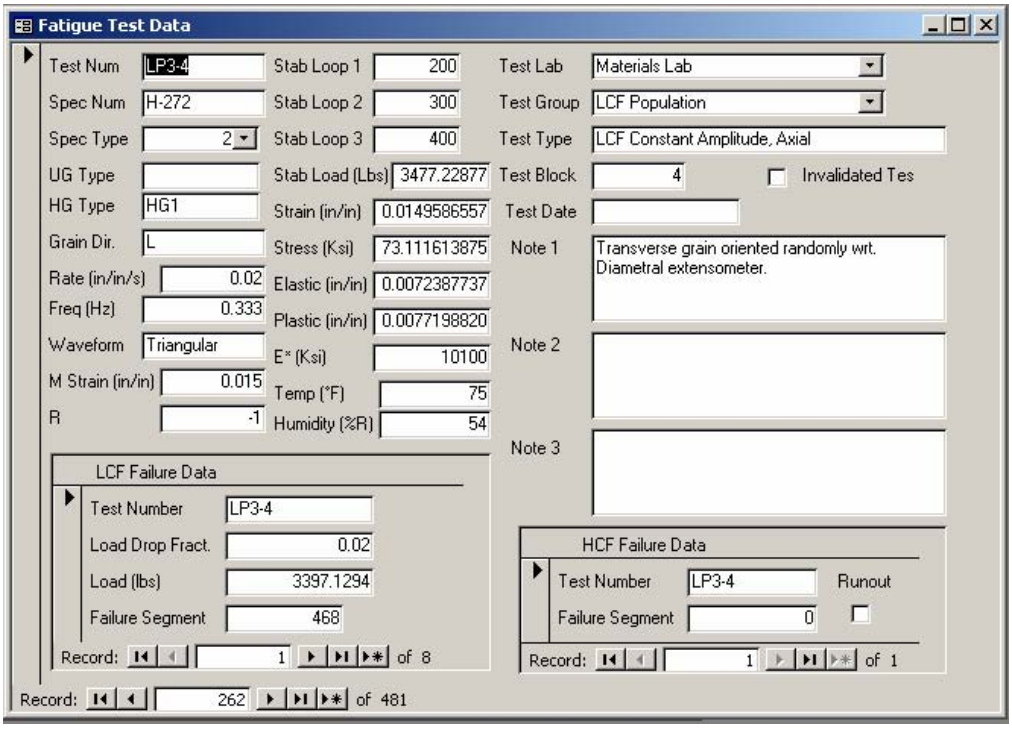

Figure 7: Example Form from 7050-T7451 Aluminum Fatigue Test Results Database

THIS PAGE INTENTIONALLY LEFT BLANK

RESULTS

TENSILE AND CYCLIC PROPERTIES

Statistical properties of the tensile test results for a sample size of 10 tests are shown in table 5, and assume a Gaussian distribution for each material property value. A complete list of tensile results for individual tests is included in appendix A.

Table 5: 7050-T7451 Tensile Properties, Based on 10 Tests

	Young's Modulus (Ksi)	Yield Stress 0.2% (Ksi)	Tensile Strength (Ksi)	Elongation[a] (%)	Area Reduction (%)
Mean	10,050	67.1	76.0	15.61	41.4
Std. Dev.	30.4	0.785	0.260	0.418	1.49
COV	0.303%	1.17%	0.342%	4.72%	3.60%

[a]1.0 in. gage length

Monotonic stress-strain curves from the 10 tensile tests show no significant variation in shapes when plotted together. Likewise, the cyclic stress-strain curves from the 10 incremental step tests show no significant variation in shape when plotted together. The resulting stabilized cyclic stress-strain curve is compared to the monotonic stress-strain curve in figure 8, and shows only a slight amount of cyclic softening at strain amplitudes below 1.6%.

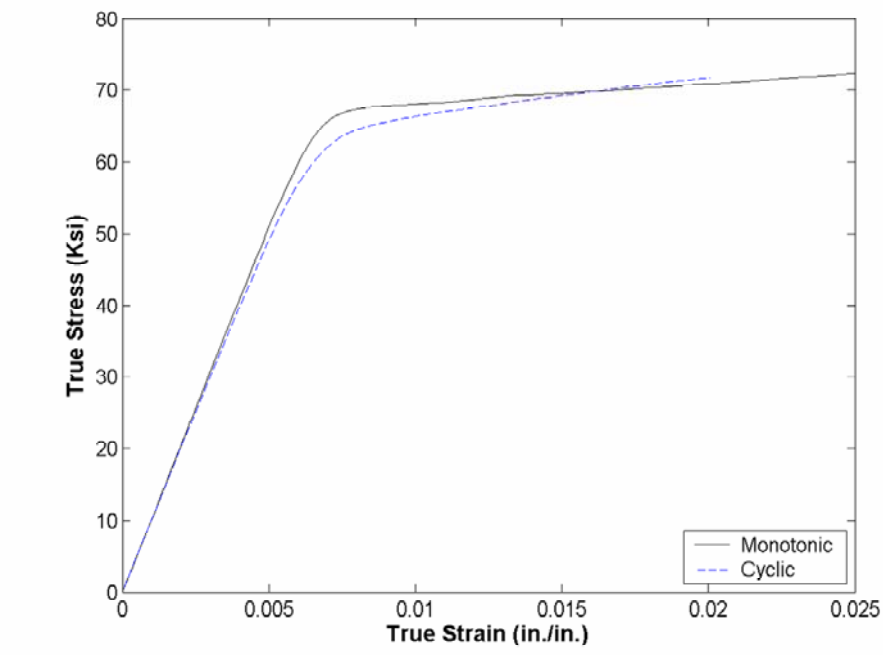

Figure 8: 7075-T7451 Monotonic and Cyclic Stress-Strain Curves

STRAIN-LIFE TEST RESULTS

Two test laboratories were used to conduct constant-amplitude strain-life tests for this research effort, primarily to reduce total testing time due to the large number of coupons to be tested. To examine the effect of lab-to-lab test variation on life scatter, an initial Uniformity Trial was performed using hourglass and uniform gage coupons at two different strain amplitudes. Statistical analyses of the results are shown in table 6, with the raw test results listed in appendix A. The life scatter was assumed to fit a base 10 lognormal distribution.

Table 6: Uniformity Trial Statistics for UG1 and HG1 Coupons, 2.0% Peak Load Drop Life

Test Lab	Strain Amp. (in./in.)	Specimen Type	Sample Size	Median ($2N_f$)	Log_{10} Median % Diff.	Log_{10} S.D. ($2N_f$)	Lab % Diff.
4.3.4.2	0.008	UG1	5	2168		0.0366	
		HG1	15	2663		0.0740	
	0.010	UG1	5	1159		0.0515	
		HG1	15	1522		0.0794	
Metcut	0.008	UG1	3	1744	-2.83	0.0505	40.0
		HG1	14	2709	0.22	0.0681	-7.97
	0.010	UG1	3	1120	-0.49	0.0252	-51.1
		HG1	15	1676	1.32	0.0990	24.7

The effect on coupon life scatter of controlling grain orientation with respect to diametral extensometer placement is shown in table 7. The data are a combination of results from several different strain-controlled test groups, but all tests were conducted in the 4.3.4.2 test lab on HG1 coupons. The differences in life scatter are shown graphically in figure 9 for total strain amplitudes, and in figure 10 for elastic and plastic strain amplitudes. The raw test results data are listed in appendix A. Stabilized elastic and plastic strain amplitude values for all tests were determined by an average of three measurements taken from hysteresis loop segments at approximately half the coupon test life.

Table 7: 4.3.4.2 Strain-Controlled Tests of HG1 Coupons, Random and Controlled Grain Orientations, 2.0% Load Drop Failure

Strain Amp. (in./in.)	Test Group	Test Type	Sample Size	Median ($2N_f$)	Log_{10} Median % Diff.	Log_{10} S.D. ($2N_f$)	S.D. % Diff.
0.006	IP1	Random Grain	10	8216	-0.97	0.0920	50.8
	IPG1	Grain Control	5	8973		0.0610	
0.007	IP1	Random Grain	10	3607	-2.33	0.0641	91.9
	IPG1	Grain Control	5	4387		0.0334	
0.008	UB	Random Grain	15	2663	-2.71	0.0740	387
	LPGA1	Grain Control	5	3316		0.0152	
0.010	UB	Random Grain	15	1522	-3.06	0.0749	6.39
	LPGA1	Grain Control	5	1918		0.0704	
0.012	LP3	Random Grain	10	1028	-3.56	0.0771	117
	LPG1	Grain Control	5	1328		0.0355	
0.015	LP3	Random Grain	10	616	-4.59	0.113	549
	LPG1	Grain Control	5	839		0.0174	
0.020	LP3	Random Grain	10	342	-5.93	0.0976	693
	LPG1	Grain Control	5	494		0.0123	
0.030	LP3	Random Grain	9	146	-6.20	0.0930	124
	LPG1	Grain Control	5	203		0.0415	
0.040	LP3	Random Grain	10	104	-3.32	0.0963	598
	LPG1	Grain Control	5	122		0.0138	

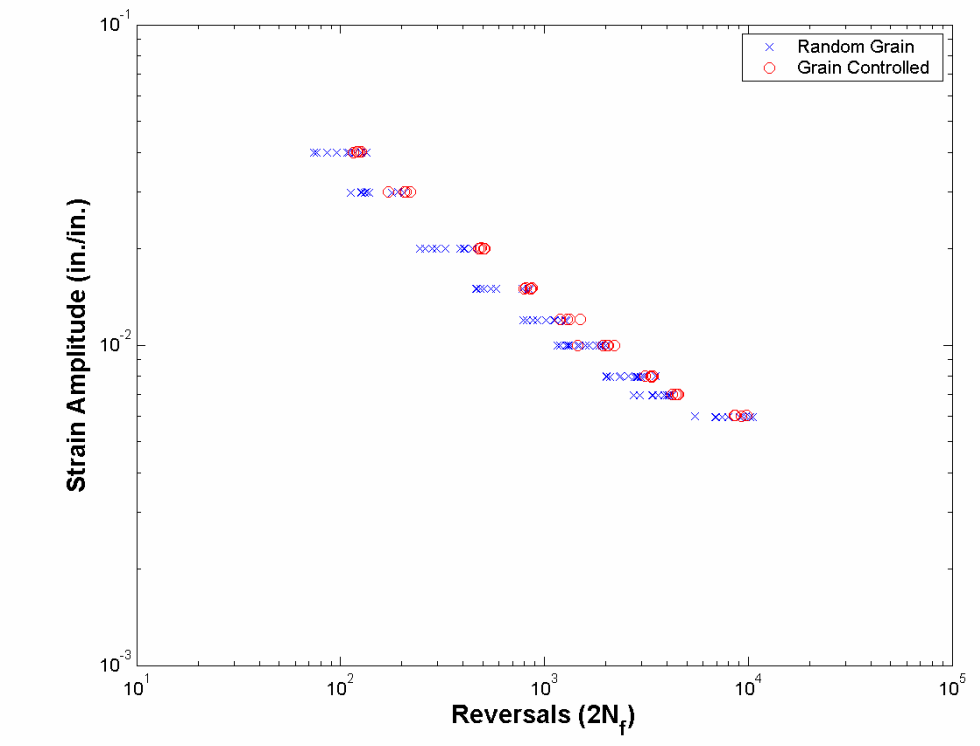

Figure 9: Strain-Life Scatter of 4.3.4.2 HG1 Coupons, Random and Controlled Grain Orientations, 2.0% Load Drop Failure

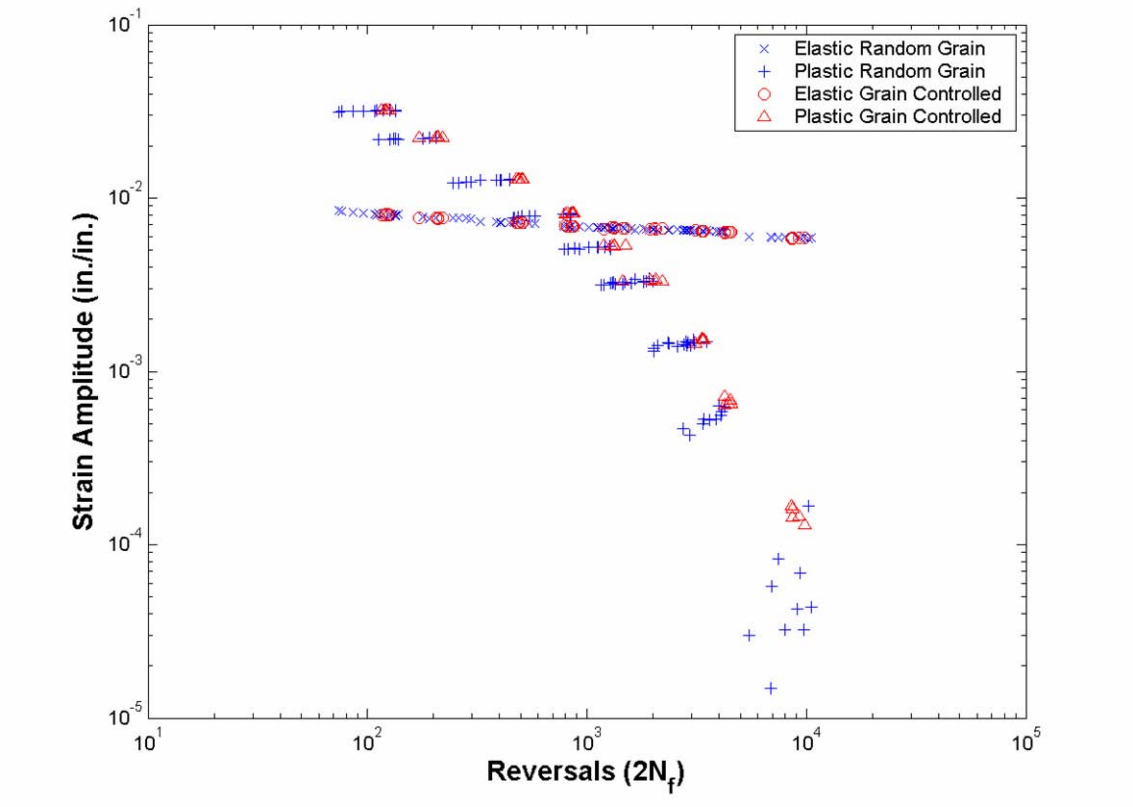

Figure 10: Elastic and Plastic Strain-Life Scatter of 4.3.4.2 HG1 Coupons, Random and Controlled Grain Orientations, 2.0% Load Drop Failure

The difference in life scatter due to the use of uniform gage versus hourglass coupon geometry is shown in table 8. The data are a combination of results from several different strain-controlled test groups, but all tests were conducted by Metcut on UG3 and HG1 coupons. All of the HG1 coupons were tested with controlled grain orientations. The differences in life scatter are shown graphically in figure 11 for total strain amplitudes, and in figure 12 for elastic and plastic strain amplitudes. The raw test results data are listed in appendix A.

Table 8: Metcut Strain-Controlled Tests of UG3 and HG1 Grain Controlled Coupons, 2.0% Load Drop Failure

Strain Amp. (in./in.)	Test Group	Coupon Type	Sample Size	Median ($2N_f$)	Log_{10} Median % Diff.	Log_{10} S.D. ($2N_f$)	S.D. % Diff.
0.006	IPUG	UG3	1	8479	-3.69	-	
	IPG2	HG1	15	11986		0.0455	
0.007	IPUG	UG3	9	3561	-5.21	0.0441	-4.54
	IPG2	HG1	15	5582		0.0462	
0.008	LPUG	UG3	4	2515	-3.99	0.0720	19.8
	LPGA2	HG1	14	3481		0.0601	
0.010	LPUG	UG3	5	1094	-8.76	0.0472	53.7
	LPGA2	HG1	15	2141		0.0307	
0.012	LPUG	UG3	4	560.5	-13.5	0.0371	24.1
	LPG2	HG1	15	1510		0.0299	
0.015	LPUG	UG3	3	346.4	-15.2	0.0443	47.2
	LPG2	HG1	15	987.9		0.0301	
0.020	LPUG	UG3	2	190.1	-17.2	0.0404	66.9
	LPG2	HG1	15	563.9		0.0242	
0.030	LPG2	HG1	14	239.7		0.0153	
0.040	LPG2	HG1	15	138.0		0.0117	

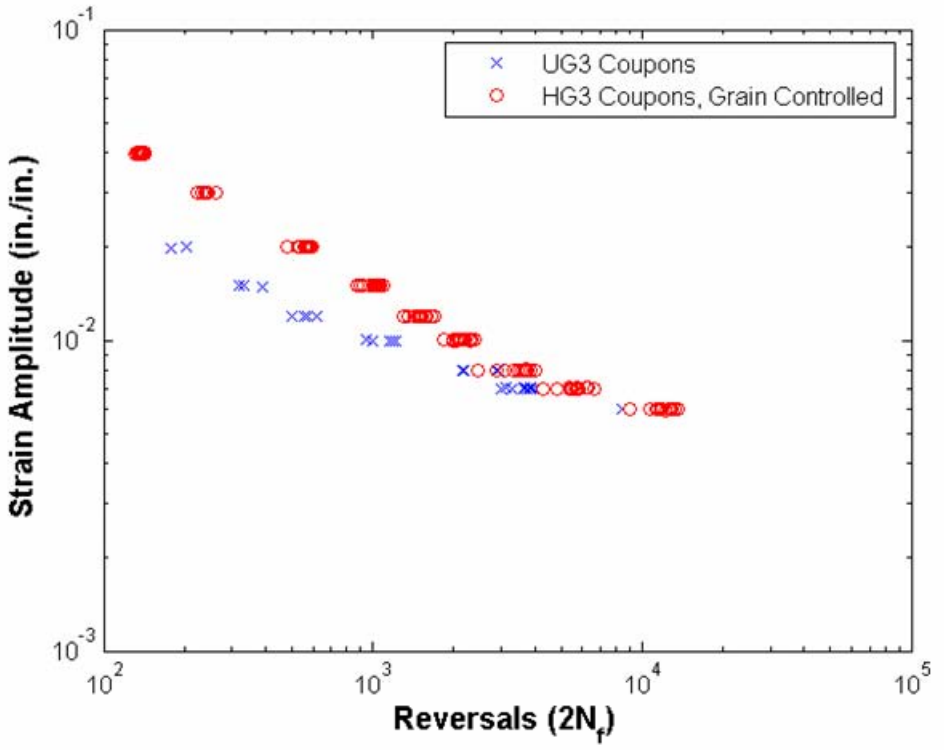

Figure 11: Strain-Life Scatter of Metcut UG3 and HG1 Controlled Grain Orientation Coupons, 2.0% Load Drop Failure

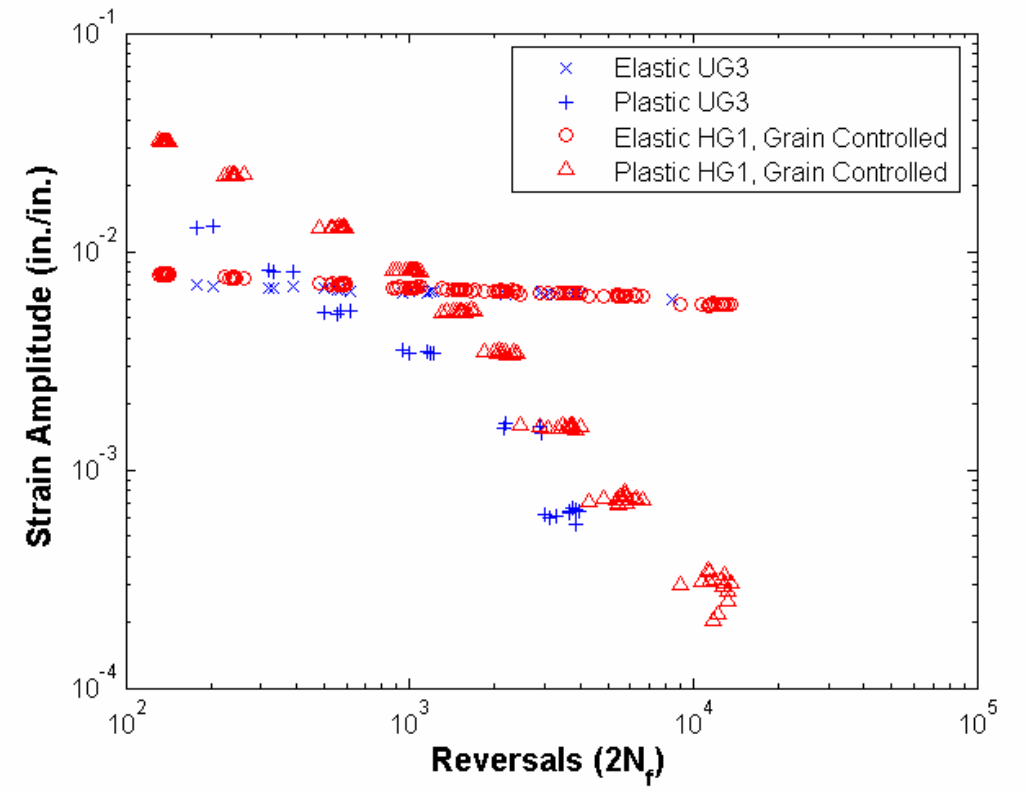

Figure 12: Elastic and Plastic Strain-Life Scatter of Metcut UG3 and HG1 Controlled Grain Orientation Coupons, 2.0% Load Drop Failure

A more extensive analysis of the effect of lab-to-lab test variation on life scatter can be demonstrated by comparing the results of the HG1 hourglass tests performed under controlled grain orientation from the two test labs. The difference in life scatter from the two test labs is shown in table 9. The differences in life scatter are shown graphically in figure 13 for total strain amplitudes, and in figure 14 for elastic and plastic strain amplitudes.

Table 9: 4.3.4.2 and Metcut Strain-Controlled Tests of HG1 Coupons, Controlled Grain Orientations, 2.0% Load Drop Failure

Strain Amp. (in./in.)	Test Group	Test Lab	Sample Size	Median ($2N_f$)	Log_{10} Median % Diff.	Log_{10} S.D. ($2N_f$)	S.D. % Diff.
0.006	IPG2	Metcut	15	11986	3.18	0.0455	-25.4
	IPG1	4.3.4.2	5	8973		0.0610	
0.007	IPG2	Metcut	15	5582	2.87	0.0462	38.3
	IPG1	4.3.4.2	5	4387		0.0334	
0.008	LPGA2	Metcut	14	3481	4.98	0.0601	295
	LPGA1	4.3.4.2	5	3316		0.0152	
0.010	LPGA2	Metcut	15	2141	1.46	0.0307	-56.4
	LPGA1	4.3.4.2	5	1918		0.0704	
0.012	LPG2	Metcut	15	1510	1.79	0.0299	-15.8
	LPG1	4.3.4.2	5	1328		0.0355	
0.015	LPG2	Metcut	15	987.9	2.43	0.0301	73.0
	LPG1	4.3.4.2	5	839		0.0174	
0.020	LPG2	Metcut	15	563.9	2.13	0.0242	96.7
	LPG1	4.3.4.2	5	494		0.0123	
0.030	LPG2	Metcut	14	239.7	3.13	0.0153	-63.1
	LPG1	4.3.4.2	5	203		0.0415	
0.040	LPG2	Metcut	15	138.0	2.57	0.0117	-15.2
	LPG1	4.3.4.2	5	122		0.0138	

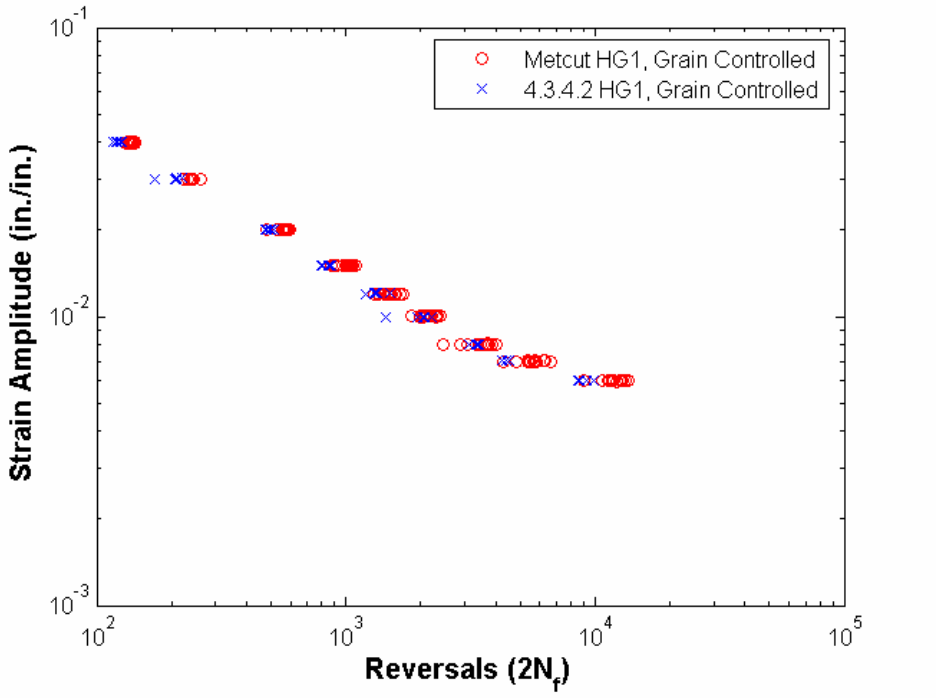

Figure 13: Strain-Life Scatter of 4.3.3.1 and Metcut HG1 Controlled Grain Orientation Coupons, 2.0% Load Drop Failure

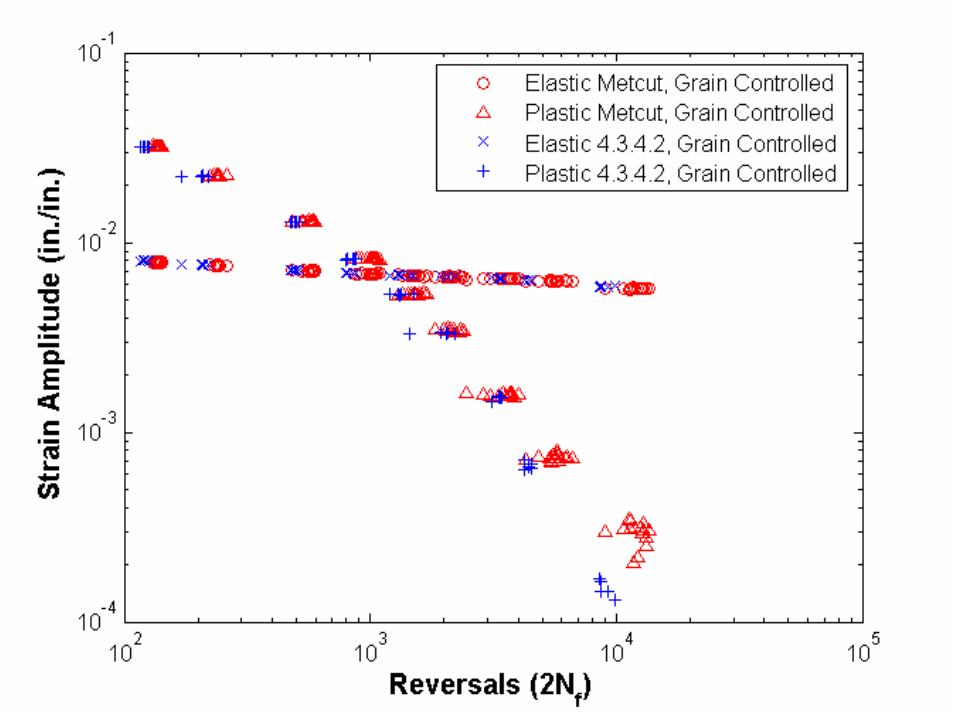

Figure 14: Elastic and Plastic Strain-Life Scatter of 4.3.4.2 and Metcut HG1 Controlled Grain Orientation Coupons, 2.0% Load Drop Failure

Load-controlled fatigue tests were performed by 4.3.4.2 and Metcut test labs on HG1 coupons, with the life scatter statistics shown in table 10. The runout limit criteria for all tests was specified as $1x10^7$ cycles. Statistics for the strain amplitude value with both failures and runouts were derived using the maximum likelihood solution for a lognormal distribution with right-censored data. The differences in life scatter are shown graphically in figure 15. The raw test results data are listed in appendix A.

Table 10: 4.3.4.2 and Metcut Load-Controlled Tests of HG1 Coupons, Initial Overstrained

Strain Amp. (in./in.)	Test Group	Test Lab	Sample Size	Run-outs	Median ($2N_f$)	Log_{10} Median % Diff.	Log_{10} S.D. ($2N_f$)	S.D. % Diff.
0.005	HP2	Metcut	15	0	30790	0.92	0.0381	52.4
	HP1	4.3.4.2	15	0	28010		0.0250	
0.004	HP2	Metcut	15	0	77180	-0.43	0.0511	5.14
	HP1	4.3.4.2	15	0	80990		0.0486	
0.003	HP2	Metcut	14	0	$4.478x10^5$	3.52	0.140	113
	HP1	4.3.4.2	15	0	$2.878x10^5$		0.0657	
0.0027	HP2	Metcut	10	1	$4.473x10^6$	-	0.463	-
0.0025	HP2	Metcut	3	3	$> 1x10^7$	-	-	-
	HP1	4.3.4.2	10	0	$7.485x10^5$	-	0.102	-
0.0022	HP1	4.3.4.2	1	0	$1.370x10^6$	-	-	-
0.002	HP1	4.3.4.2	5	5	$> 1x10^7$	-	-	-

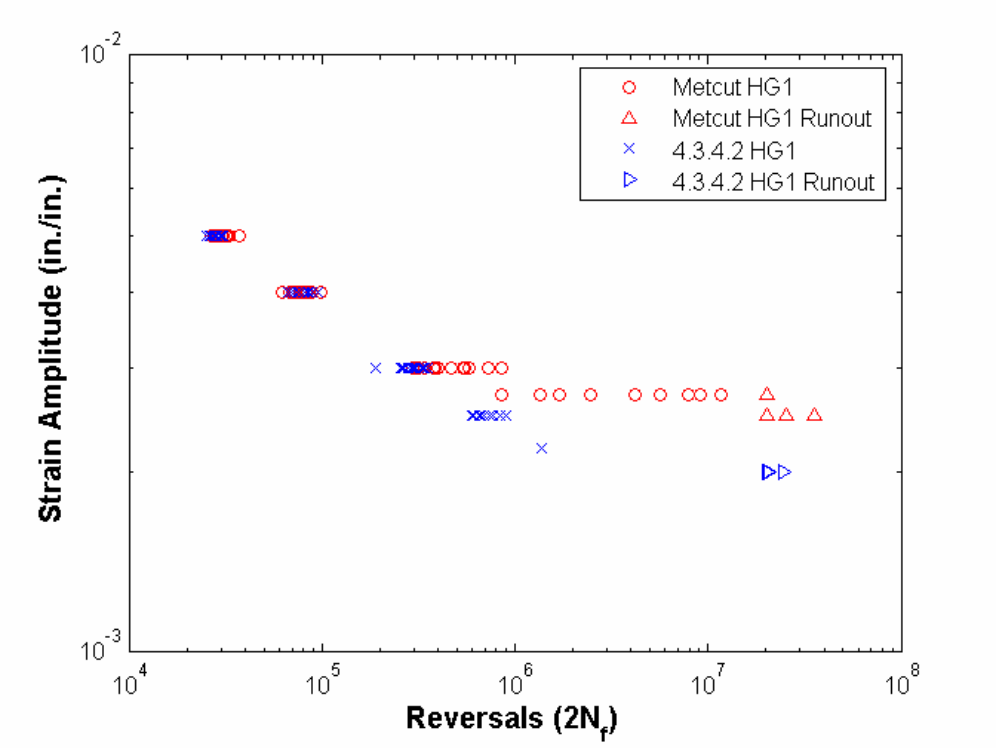

Figure 15: Strain-Life Scatter of 4.3.3.1 and Metcut HG1 Coupons, Initial Overstrained

The difference in life scatter due to the use of uniform gage versus hourglass coupon geometry in load-controlled tests is shown in table 11. All tests for this data set were conducted by Metcut on UG3 and HG1 coupons. The runout limit criteria for all tests was specified as $1x10^7$ cycles. Statistics for the strain amplitude value with both failures and runouts were derived using the maximum likelihood solution for a lognormal distribution with right-censored data. The differences in life scatter are shown graphically in figure 16. The raw test results data are listed in appendix A.

Table 11: Metcut Load-Controlled Tests of HG1 and UG3 Coupons, Initial Overstrained

Strain Amp. (in./in.)	Test Group	Test Lab	Sample Size	Run-outs	Median ($2N_f$)	Log_{10} Median % Diff.	Log_{10} S.D. ($2N_f$)	S.D. % Diff.
0.005	HP2	Metcut	15	0	30790	0.20	0.0381	-41.2
	HPUG	Metcut	12	0	30163		0.0648	
0.004	HP2	Metcut	15	0	77180	-0.99	0.0511	2.82
	HPUG	Metcut	9	0	86351		0.0497	
0.003	HP2	Metcut	14	0	$4.478x10^5$	-2.48	0.140	-52.1
	HPUG	Metcut	12	0	$6.235x10^5$		0.292	
0.0027	HP2	Metcut	10	1	$4.473x10^6$	-	0.463	-
0.0025	HP2	Metcut	3	3	$> 1x10^7$	-	-	-
	HPUG	Metcut	14	8	$4.316x10^7$	-	1.319	-

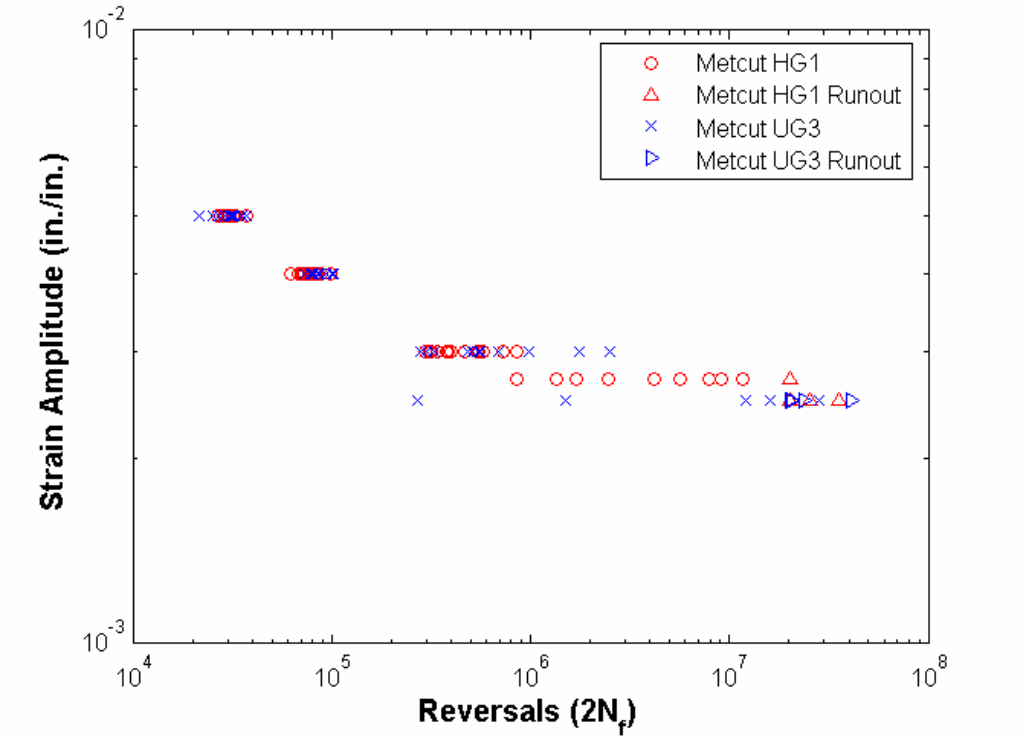

Figure 16: Strain-Life Scatter of Metcut HG1 and UG3 Coupons, Initial Overstrained

DISCUSSION

COUPON TEST PROCEDURES

A nominal grip diameter of 0.50 in. is specified for the type of hydraulic collet used to hold the fatigue coupons during testing. All of the coupons cut from Plate 1 had a nominal grip diameter of 0.485 in. because the plate thickness was only 0.50 in., and did not leave any material for machining to the preferred grip dimension. The resulting dimensional mismatch between the coupons and collets caused some coupons to pull out of the grips during testing, and made load train alignment difficult. The solution was to fabricate 17-4 PH Stainless Steel collars with a 0.485 in. inside diameter, and a 0.75 in. outside diameter, which slip over the grip section of the coupon and fit the next larger hydraulic collet size. This eliminated the problem of coupons being pulled out of the grips during testing, and significantly improved load train alignment from test to test. Metcut standard test procedures also specify the use of steel collars with hydraulic collet grips, and were used on all tests performed for NAVAIR.

The ratio of reduced cross-sectional length to nominal diameter on cylindrical uniform gage coupons is important in determining the compressive buckling resistance of the coupons. Reference 4 specifies an acceptable range of reduced cross-sectional length from two to four times the nominal diameter (aspect ratio). During testing, the UG1 coupon with an aspect ratio of 4 could absorb no more that 1.5% in./in. compressive strain without discernable signs of buckling. The UG2 coupons, with an aspect ratio of 2.67, were able to go to 2.0% in./in. compressive strain without buckling. UG3 coupons with an aspect ratio of 3.0 were also able to achieve 2.0% in./in. compressive strain without buckling. The buckling performance of the uniform-gage coupon geometries tested here may differ somewhat for different materials, and should be carefully considered when developing strain-life test matrices. The HG1 hourglass coupons experienced no discernable buckling for any tests conducted at 4.0% in./in. compressive strain or lower.

INCREMENTAL STEP TESTS

The traditional method of deriving a cyclic stress-strain curve for a material is to plot the stabilized hysteresis loops from a series of fully reversed, constant amplitude strain-life tests on uniform gage coupons with various peak strain values. Connecting the loop tips gives a trace of the stabilized cyclic stress-strain curve for the material. The incremental step test is a much faster method of obtaining a cyclic stress-strain curve, since only one test is required. For the 7050-T7451 material tested here, the traditional method and the incremental step method give slightly different results, as shown in figure B-1. To derive a hysteresis loop from a cyclic stress-strain curve, Massing postulated that a stabilized hysteresis curve was simply twice the cyclic stress-strain curve (reference 20). Plotting hysteresis loops derived from the incremental step cyclic stress-strain curve with stabilized hysteresis loops from uniform gage test specimens provides a measure of how closely 7050-T7451 aluminum fits Massing's hypothesis. These results are plotted in figures B-2 to B-7, and show a significant difference in loop shape at peak strains above 0.8% in./in.

Another method of viewing the loop shape difference is by shifting all of the compressive peaks to the origin of a single plot. The difference in hysteresis loop shapes between the two methods can easily be seen by comparing figures B-8 and B-9. The uniform gage test data indicate that the proportional (elastic) strain range decreases as the peak strain value of the test increases, thus violating Massing's material behavior model. Jhansale and Topper (reference 21) demonstrated that the hysteresis loops shapes can be extracted from a single curve by shifting the loop along the elastic slope so that the upper branches of the loops are overlaid on each other (figure B-10). This yields a stress-strain curve shape that is consistent for all of the loops, but the variation in proportional stress must be included in any hysteresis loop calculation. To include the proportional stress variation in a strain-life model, a history-dependent material model that includes all transient effects must be utilized. This would significantly increase the complexity of the strain-life analysis. As a result, the cyclic stress-strain curve from the incremental step tests should be used for life predictions, since it already incorporates some of the material's transient behavior effects due to the variable loading used in the test.

STRAIN-LIFE TEST PROCEDURES

During strain-life testing of hourglass coupons, it became apparent that the placement of the diametral strain gage on the test coupon has a significant effect on the resulting fatigue life scatter. Examination of the Uniformity Trial statistics in table 6 show that the hourglass HG1 coupons exhibit higher mean fatigue lives than the uniform gage UG1 coupons, but significantly more scatter. By plotting the stress-life results for a single strain amplitude of these tests (figure C-1), it can be seen that there is a strong correlation between the stabilized stress amplitude and fatigue life for the hourglass coupons. As the cyclically-stabilized stress amplitude decreases, the fatigue life significantly increases. This trend becomes more pronounced for larger strain amplitudes where more plasticity is present.

Microstructural examination of coupons cut from Plate 1 shows a preferred grain orientation in the material due to rolling of the thin plate (figures C-2 and C-3). Since test coupons were cut with their loading direction parallel to the rolling direction of the plate, this preferred grain orientation exists through the cross-section of all the test coupons. Two hourglass coupons from test group LP3 were selected for post-test microstructural analysis to determine the grain orientation with respect to the diametral extensometer contact points. The two coupons selected represent the approximate minimum (H-865) and maximum (H-840) extremes in fatigue life for the set of coupons tested at 3.0% strain amplitude in the group (table 12). Since none of the test coupons had plate orientation markers machined into them during fabrication, the two fractured coupons had their grip ends polished and etched to determine grain orientation. This was matched up against the fretting marks left by the diametral extensometer contact pads in the gage section of the coupons. The result was that the coupon with the short fatigue life had the extensometer placed in the long-transverse (LT) direction, and the coupon with the long fatigue life had the extensometer placed in the short-transverse (ST) direction (figure C-4).

Table 12: Grain Orientation Effect on Fatigue Life of HG1 Hourglass Coupons, LP3 Test Group

Coupon	Strain Amp. (%)	Grain Orientation	Poisson's Ratio Constant	Stress Amp. (Ksi)	Plastic Strain (%)	2.0% Load Drop Life
H-865	3.0	LT	0.33	82.9	2.18	112
H-429	3.0	LT	0.297	82.4	2.18	112
H-840	3.0	ST	0.33	76.9	2.24	192
H-603	3.0	ST	0.317	76.7	2.24	222

To verify these results, and to investigate the effect of changing the elastic Poisson's ratio, two additional coupons (H-429 and H-603) were microstructurally examined and had their grain orientations marked prior to testing. Before fatigue testing, the coupons were cycled elastically and the elastic Poisson's ratios were tuned to give the same load versus diametral strain relation as recorded in the first segment of the H-804 and H-865 fatigue tests. These test results are listed in table 12, and also show the elastic Poisson's ratio values used in the diametral to axial strain conversion equation for each test. The stress amplitudes and fatigue lives for the tests are consistent for their respective grain orientations, and also show that varying the elastic Poisson's ratio used to control the test has no significant effect on the results. The only meaningful effect of reducing the test Poisson's ratio was a slight increase in the hysteresis loop elastic modulii, and a slight reduction in total strain values in the nonlinear region.

In an effort to quantify the true elastic Poisson's ratio for the test coupons, five UG1 coupons were microstructurally examined and had their grain orientations marked. Axial and diametral extensometers were attached, and the elastic Poisson's ratio was determined in both the ST and LT grain orientations for the coupons at room temperature. The coupons were then cycled under constant-amplitude axial extensometer strain control at a strain-amplitude of 1.0% (in./in.), R = -1 for 150 cycles. The elastic Poisson's ratio was then recalculated for both grain orientations in the coupons. The tests were conducted in accordance with the guidelines in ASTM E132 (reference 22), except that the geometry of the UG1 coupons is outside the scope of the specification. Both tensile and compressive Poisson's ratios were calculated, with the values averaged and presented in table 13. Grouping all measurements into a single average value for each grain orientation gives a Poisson Ratio of 0.32 for the LT direction and 0.35 for the ST direction. This variation from the nominal 0.33 is on the order of the variation used in the tests of table 12.

Table 13: Elastic Poisson's Ratios for Coupon LT and ST Grain Orientations

Coupons	Poisson's Ratio (LT Direction)		Poisson's Ratio (ST Direction)	
	Prefatigue	Postfatigue	Prefatigue	Postfatigue
94	0.33	0.32	0.35	0.35
122	0.32	0.32	0.34	0.35
196	0.32	0.32	0.34	0.34
210	0.32	0.32	0.34	0.35
296	0.33	0.33	0.35	0.36

Plotting cyclically stabilized hysteresis loops for various test configurations shows how grain orientation affects loop shape. Figures C-5 through C-10 compare UG3 uniform gage hysteresis loops with loops from the minimum life coupon tests of HG1 hourglass coupons with random grain orientation, and loops from HG1 hourglass coupons tested with the diametral extensometer in the ST grain direction. Choosing the minimum life test from a sample size of 15 random grain orientation tests (Test Groups LP3, UB, and IP1) at a given strain amplitude is assumed to give a coupon with the diametral extensometer placed in the LT direction, based on the previous grain analysis results at 3.0% strain amplitude. Coupons tested with the diametral extensometer in the ST grain direction (Test Groups LPG1, LPGA1, and IPG1) were first polished at the grip end to determine microstructure grain orientation, and then set up with the specified extensometer orientation prior to test. The results in figures C-5 through C-10 show that hourglass coupons tested in the ST grain orientation have hysteresis loops that match much more closely the loops from uniform gage coupons. The difference in stress range between the hourglass coupons tested in the LT grain orientation and the other test configurations increases as the strain amplitude increases. At strain amplitudes below 0.7%, the difference in hysteresis loop shape between the three test configurations is not significant. Based on these results, hourglass coupons tested in the ST grain orientation are assumed to more accurately replicate the strain-life test response of uniform gage coupons.

Coupons tested with the diametral extensometer in the ST grain direction are categorized as grain-controlled hourglass tests in the test matrix of table 4. The scatter in stress-life results for the UG3 uniform gage, random grain orientated and grain-controlled hourglass coupons is shown in figures C-11 through C-19 for specific test strain amplitudes. These plots show the same trends observed in the hysteresis loop plots, but also show the relative scatter for all of the coupons tested. For load-controlled HG1 hourglass coupons with initial overstraining, the effect of diametral extensometer placement with respect to the material grain orientation for the overstraining sequence was not considered significant enough to affect the remaining fatigue life of the coupon tests. Therefore, all of the load-controlled HG1 hourglass coupon tests had their grain directions oriented randomly with respect to the diametral extensometer for the initial overstrain portion of the tests.

STRAIN-LIFE TEST RESULTS

Strain-controlled results from uniform gage coupon tests UG3 show that the elastic modulus changes depending on the amount of plastic straining occurring in the test. For fully reversed, purely elastic cycling, the tensile modulus is equivalent to the monotonic value. As the amount of plastic straining is increased, the elastic modulus upon release of loading decreases for larger and larger values of plastic strain. Examples of this effect are shown in table 14 for selected coupon results. Each modulus value is an average of three measurements taken from hysteresis loop segments at approximately half the coupon test life.

Table 14: Elastic Modulus Variation for Strain-Controlled UG3 Coupon Tests

Strain Amp. (%)	Coupon	Elastic Modulus-ascending loop (Ksi)	Elastic Modulus-descending loop (Ksi)	Elastic Modulus-average (Ksi)
0.6	IPUG-10	10,563	10,268	10,416
0.7	IPUG-1	10,103	10,107	10,105
0.8	LPUG-22	9,953	9,653	9,803
1.0	LPUG-27	9,692	9,490	9,591
1.2	LPUG-12	9,358	9,339	9,349
1.5	LPUG-29	9,064	9,071	9,068
2.0	LPUG-33	8,628	8,994	8,811

Use of the cyclic elastic modulus value of 10,100 Ksi. from table 3 to calculate plastic strains results in lower predicted plastic strain values than actual for strain amplitudes below 0.7% in./in. For strain amplitudes above 0.7% in./in., the amount of plastic strain is overpredicted compared to the actual values. The magnitude of plastic strain error is only significant at strain amplitudes with small amounts of plasticity, where it is possible to calculate negative plastic strain values. For this investigation, any coupons with calculated plastic strain values less than zero were reset to a small positive value.

Results for the Uniformity Trial tests in table 6 show that HG1 hourglass coupons tested with random grain orientations have a higher mean, but more scatter than the UG1 uniform gage coupons tested. Interlaboratory variation in $\log_{10}$ median life for the coupon geometries tested is less than 3.0%, with most coupon-strain amplitude combinations less than 1.4%. Interlaboratory variation in $\log_{10}$ standard deviation ranges from 8% to 25% for hourglass coupons, but is significantly greater for uniform gage coupons primarily due to the small test sample size.

The effect on coupon life of controlling microstructure grain orientation with respect to diametral extensometer placement shown in table 7 is that the controlled grain orientation tests have an increase in median life over random grain oriented tests, but significantly less scatter. Controlling grain orientation also significantly reduces the scatter in plastic strain values at lower total strain amplitudes (figure 10).

The difference in life scatter for uniform gage and grain-controlled hourglass coupon tests shown in table 8 is a decrease in $\log_{10}$ median life of 3% to 17% for the uniform gage coupons, but a general increase in $\log_{10}$ standard deviation of between 20% to 67%. It should be noted that many of the test strain amplitudes had small sample sizes of UG3 uniform gage coupon results to draw statistics from. Ten samples of uniform gage coupons were tested at each strain amplitude from 0.6% to 2.0% strain, but many coupons failed due to cracking at the axial extensometer contact location, and were invalidated.

The more extensive analysis of interlaboratory test variation shown in table 9 indicates that for grain-controlled HG1 hourglass coupons, the Metcut tests have an increased $\log_{10}$ median life of between 1.5% and 5%. The magnitude of $\log_{10}$ standard deviation values vary from 15% to nearly 300%, with neither lab having consistently higher or lower values for the strain range

tested. This would indicate that the test sample sizes are insufficient to distinguish any significant difference in coupon life scatter between the two labs, especially in the case of the 4.3.4.2 Lab test results.

Load-controlled fatigue tests of HG1 hourglass coupons from table 10 show no significant difference in $\log_{10}$ median life values above 0.3% strain amplitude. An apparent difference in fatigue endurance limit between the two test labs affects the life scatter in strain amplitudes of 0.3% and lower, so that significant variation is seen in the $\log_{10}$ median life and the $\log_{10}$ standard deviation values.

The difference in life scatter for uniform-gage and hourglass coupons in load-controlled tests shown in table 11 is a small decrease in $\log_{10}$ median life at 0.3% strain amplitude for the uniform gage coupons, but a general increase in $\log_{10}$ standard deviation values over the strain ranges tested. Changes in $\log_{10}$ median life values are due primarily to a slight decrease in fatigue endurance limit of the uniform gage coupons, with the difference being much smaller than that shown in the interlaboratory load-controlled hourglass tests of table 10. This demonstrates that for this material, the choice of coupon geometry is less important in determining fatigue endurance limit than the laboratory doing the testing. Coupon geometry is important, however, in determining the amount of scatter in the load-controlled fatigue life results.

CONCLUSIONS

A properly characterized, probabilistic strain-life curve of material fatigue strength is essential for reliability-based fatigue life predictions of aircraft components. This investigation shows that the choice of coupon geometry, test procedures, and the test laboratory all have an effect on the statistics of the strain-life test results. The most important variable in determining the fatigue life scatter of strain-controlled tests is in the choice of coupon geometry. The use of an hourglass coupon geometry also requires attention to the microstructure of the base material used to fabricate the coupons. If a preferred grain orientation exists in the material, strain-life test procedures must be utilized that will control the diametral extensometer location with respect to the grain direction. For the 0.50 in. thick 7050-T7451 aluminum plate investigated here, orienting the diametral extensometer in the ST grain direction of the test coupons resulted in stress amplitude values and hysteresis loop shapes that are much closer to uniform gage coupon test results.

For strain-controlled tests, uniform gage coupon lives have less mean, and less scatter than hourglass coupons tested with a random grain orientation. Compared to hourglass coupons tested with the grain orientation controlled, uniform gage coupon lives have less mean, but more scatter. For the sample sizes tested, there was no consistent difference in the strain-life results scatter generated by the two test labs. In the load-controlled tests results, there was no significant difference between the two coupon types in the finite life region, but the endurance limit for the uniform gage coupon was slightly lower. There was also no significant variation in the load-controlled results between test labs, except that the endurance limits were somewhat different. This difference was less than that due to coupon geometry. It should be noted that sample size is an important consideration in trying to distinguish between populations of strain-life test results from different coupon geometries and test labs. In several cases in this investigation, sample sizes were insufficient to clearly distinguish differences in population variances. Further statistical analysis of the test results is necessary to better define the test sample sizes needed to fully capture the variation in material fatigue resistance, especially with regard to the fitting of probabilistic strain-life curves. Although not considered to be significant in these tests, interlaboratory variation in fatigue results may still be important for other laboratories or material systems. However, it may be prohibitively expensive to conduct a proper interlaboratory test program for probabilistic strain-life properties, given the large number of samples required to clearly define population variances.

THIS PAGE INTENTIONALLY LEFT BLANK

REFERENCES

1 Dowling, N.E., “Mechanical Behavior of Materials, Second Ed.,” Prentice Hall, Upper Saddle River, NJ, 1999.

2 “Fatigue Under Complex Loading: Analyses and Experiments,” Wetzel, R.M. Ed., Society of Automotive Engineers, Inc., Warrendale, PA, 1977.

3 Morrow, J.D., Martin, J.F., and Dowling, N.E., “Local Stress-Strain Approach to Cumulative Fatigue Damage Analysis, Final Report,” UILU-Eng 74 6001, T. & A. M. Report No. 379, Department of Theoretical and Applied Mechanics, University of Illinois, Urbana, IL, Jan 1974.

4 ASTM E606, “Standard Practice for Strain-Controlled Fatigue Testing,” American Society for Testing and Materials.

5 ASTM E8, “Standard Test Methods for Tension Testing of Metallic Materials,” American Society for Testing and Materials.

6 ASTM E646, “Standard Test Method for Tensile Strain-Hardening Exponents (*n*-Values) of Metallic Sheet Materials,” American Society for Testing and Materials.

7 Bannantine, J.A., Comer, J.J., and Handrock, J.L., “Fundamentals of Metal Fatigue Analysis,” Prentice Hall, Englewood Cliffs, New Jersey, 1990, pp. 52-54.

8 Landgraf, R.W., Morrow, J., and Endo, T., “Determination of the Cyclic Stress-Strain Curve,” *Journal of Materials*, JMLSA, Vol. 4, No. 1, Mar 1969, pp. 176-188.

9 Military Handbook MIL-HDBK-5H, "Metallic Materials and Elements for Aerospace Vehicle Structures," Department of Defense, 1 December 1998.

10 ASTM E466, “Standard Practice for Conducting Constant Amplitude Axial Fatigue Tests of Metallic Materials,” American Society for Testing and Materials.

11 Dowling, N.E., “A Review of Fatigue Life Prediction Methods,” SAE Paper No. 871966, *SAE/DOC Symposium on Durability by Design*, Dearborn, MI, Society of Automotive Engineers, 20-21 Oct 1987.

12 Topper, T.H. and Sandor, B.I., “Effects of Mean Stress and Prestrain on Fatigue-Damage Summation,” *Effects of Environment and Complex Load History on Fatigue Life, ASTM STP 462*, American Society for Testing and Materials, 1970, pp. 93-104.

13 Dowling, N.E., “Fatigue Failure Predictions for Complicated Stress-Strain Histories,” *Journal of Materials*, JMLSA, Vol. 7, No. 1, Mar 1972, pp. 71-81.

14 Dowling, N.E., “Fatigue Life and Inelastic Strain Response under Complex Histories for an Alloy Steel,” *Journal of Testing and Evaluation*, JTEVA, Vol. 1, No. 4, Jul 1973, pp. 271-287.

15 Little, R. E., and Jebe, E. H., *ASTM STP-588, Manual on Statistical Planning and Analysis for Fatigue Experiments*, American Society of Testing and Materials, Philadelphia, PA, 1975, pp. 19-27.

16 Fields, S.S. and Meyer, E.S., “Fatigue Guidelines, Material Characterization and Data Reduction, Development of Crack Initiation Material Curves,” Boeing Report No. E0098-MET-052-QD, of 11 May 1999.

17 Dowling, N. E., "Notched Member Fatigue Life Predictions Combining Crack Initiation and Propagation," *Fatigue of Engineering Materials and Structures*, Vol. 2, 1979, pp. 129-138.

18 ASTM E468, “Standard Practice for Presentation of Constant Amplitude Fatigue Test Results for Metallic Materials,” American Society for Testing and Materials.

19 SAE J2409 Surface Vehicle Standard, “Strain-Life Fatigue Data Exchange File Format,” Society of Automotive Engineers, Jun 1998.

20 Massing, G., *Proceedings of the 2nd International Congress of Applied Mechanics*, Zurich, 1926.

21 Jhansale, H.R. and Topper, T.H., “Engineering Analysis of the Inelastic Stress Response of a Structural Metal Under Variable Cyclic Strains,” *Cyclic Stress-Strain Behavior - Analysis, Experimentation and Failure Prediction*, ASTM STP 519, American Society for Testing and Materials, 1973, pp. 246-270.

22 ASTM E132, “Standard Test Method for Poisson’s Ratio at Room Temperature,” American Society for Testing and Materials.

APPENDIX A
TEST RESULT TABULAR DATA

Table A-1: 7050-T7451 Aluminum Tensile Properties

Test	Young's Modulus (Ksi)	Yield Stress, 0.2% (Ksi)	Tensile Strength (Ksi)	True Fracture Strength (Ksi)	True Fracture Ductility (in./in.)	Elongation[a] (%)	Area Reduction (%)
ST-5	10,090	67.0	75.8	103	0.591	15.8	44.2
ST-6	10,015	67.3	76.0	101	0.528	15.7	40.4
ST-7	10,070	67.3	76.1	103	0.559	15.3	42.2
ST-8	10,101	67.9	76.6	104	0.559	15.9	42.2
ST-9	10,007	67.2	76.0	99.7	0.517	15.5	39.8
ST-10	10,026	66.8	75.6	101	0.569	16.1	42.8
ST-11	10,042	67.4	76.0	97.6	0.538	16.3	41.0
ST-12	10,047	65.0	76.3	102	0.538	15.1	41.0
ST-13	10,054	67.5	76.1	99.6	0.507	15.1	39.2
ST-14	10,052	67.4	76.2	103	0.538	15.3	41.0

Table A-2: 4.3.4.2 Uniformity Trial, UG1 Coupons

Test	Strain Amp. (%)	Stress Amp. (Ksi)	Plastic Strain Amp. (%)	Peak Load Drop Failure Life ($2N_f$)					
				2%	5%	10%	25%	50%	Fracture
UB-1	0.8	63.6	0.165	2061	2123	2143	2163	2175	2191
UB-17	0.8	64.0	0.164	2395	2541	2603	2649	2655	2663
UB-26	0.8	64.3	0.161	1933	1961	1973	1983	2001	2023
UB-34	0.8	64.1	0.163	2203	2283	2355	2439	2513	2577
UB-9	0.8	63.4	0.170	2278	2352	2378	2418	2454	2484
UB-10	1.0	64.9	0.355	1292	1360	1376	1382	1386	1388
UB-18	1.0	65.2	0.351	1187	1213	1225	1245	1267	1279
UB-2	1.0	65.1	0.350	951	975	1001	1031	1061	1069
UB-25	1.0	65.5	0.348	1157	1185	1195	1203	1209	1219
UB-33	1.0	65.0	0.353	1241	1277	1285	1291	1295	1299

Table A-3: Metcut Uniformity Trial, UG1 Coupons

Test	Strain Amp. (%)	Stress Amp. (Ksi)	Plastic Strain Amp. (%)	Peak Load Drop Failure Life ($2N_f$)					
				2%	5%	10%	25%	50%	Fracture
UC-17	0.8	63.3	0.173	1861	1929	1961	2007	2033	2034
UC-25	0.8	63.4	0.170	1525	1759	1813	1837	1857	1884
UC-33	0.8	63.3	0.171	1869	1991	2039	2071	2075	2102
UC-10	1.0	64.9	0.355	1057	1087	1099	1125	1173	1199
UC-18	1.0	64.7	0.357	1119	1249	1319	1351	1355	1364
UC-34	1.0	64.9	0.355	1187	1265	1297	1331	1389	1484

Table A-4: 4.3.4.2 Uniformity Trial, HG1 Coupons

Test	Strain Amp. (%)	Stress Amp. (Ksi)	Plastic Strain Amp. (%)	Peak Load Drop Failure Life ($2N_f$)					
				2%	5%	10%	25%	50%	Fracture
UB-11	0.8	65.7	0.147	3084	3314	3482	3678	3888	4032
UB-12	0.8	65.7	0.148	3520	3932	4166	4344	4488	4560
UB-13	0.8	66.2	0.142	2096	2174	2194	2198	2198	2198
UB-19	0.8	66.2	0.141	2972	3284	3426	3562	3606	3622
UB-20	0.8	66.3	0.141	2848	3118	3204	3238	3242	3242
UB-21	0.8	65.2	0.153	3064	3402	3590	3706	3772	3774
UB-3	0.8	65.5	0.149	2820	3054	3202	3404	3442	3500
UB-30	0.8	65.7	0.147	2876	3258	3354	3390	3418	3428
UB-31	0.8	66.8	0.137	2028	2078	2146	2178	2182	2182
UB-32	0.8	67.1	0.132	2028	2046	2054	2064	2066	2066
UB-38	0.8	65.7	0.147	2342	2544	2706	2850	2922	3040
UB-39	0.8	65.8	0.146	3098	3462	3618	3814	3868	3950
UB-4	0.8	66.0	0.144	2764	3014	3170	3314	3438	3438
UB-40	0.8	66.5	0.140	2576	2756	2768	2786	2796	2796
UB-5	0.8	65.9	0.145	2366	2554	2696	2862	2928	2928
UB-14	1.0	67.7	0.327	1318	1420	1436	1446	1448	1448
UB-15	1.0	68.1	0.321	1456	1520	1570	1608	1622	1623
UB-16	1.0	68.0	0.323	1302	1410	1444	1476	1486	1486
UB-22	1.0	67.4	0.332	1818	1984	2060	2190	2214	2238
UB-23	1.0	67.5	0.328	1484	1618	1696	1728	1742	1764
UB-24	1.0	68.2	0.322	1278	1306	1322	1334	1344	1352
UB-27	1.0	68.5	0.317	1198	1262	1288	1294	1294	1294
UB-28	1.0	67.7	0.325	1594	1766	1818	1844	1854	1862
UB-29	1.0	68.8	0.315	1158	1180	1190	1196	1196	1196
UB-35	1.0	67.4	0.329	1806	1988	2076	2204	2342	2352
UB-36	1.0	67.2	0.332	1864	2106	2228	2372	2446	2482
UB-37	1.0	68.5	0.319	1340	1356	1362	1364	1364	1364
UB-6	1.0	67.0	0.333	2002	2172	2256	2322	2336	2346
UB-7	1.0	66.3	0.341	1650	1748	1834	1942	1980	1980
UB-8	1.0	66.2	0.342	1928	2090	2174	2308	2414	2420

Table A-5: Metcut Uniformity Trial, HG1 Coupons

Test	Strain Amp. (%)	Stress Amp. (Ksi)	Plastic Strain Amp. (%)	Peak Load Drop Failure Life ($2N_f$)					
				2%	5%	10%	25%	50%	Fracture
UC-11	0.8	64.7	0.156	3179	3249	3341	3341	3449	3465
UC-12	0.8	65.7	0.147	2619	3035	3293	3293	3647	3666
UC-13	0.8	65.7	0.148	3093	3417	3619	3619	3817	3919
UC-19	0.8	65.4	0.152	2493	2887	3107	3107	3389	3399
UC-20	0.8	65.3	0.152	3155	3431	3635	3635	3969	4037
UC-21	0.8	65.9	0.147	2959	3267	3459	3459	3699	3758
UC-27	0.8	66.2	0.145	2641	3085	3093	3093	3103	3103
UC-28	0.8	65.5	0.152	2907	3523	3797	3797	4063	4200
UC-29	0.8	66.7	0.138	1807	1991	1993	1993	1993	1993
UC-3	0.8	65.2	0.152	3017	3783	3815	3815	3895	3910
UC-35	0.8	66.3	0.142	2507	2537	2545	2545	2553	2553
UC-36	0.8	66.4	0.141	2579	2709	2791	2791	2883	2883
UC-37	0.8	66.9	0.137	2279	2297	2301	2301	2303	2303
UC-4	0.8	65.9	0.146	3099	3331	3495	3495	3629	3629
UC-14	1.0	68.5	0.321	1235	1247	1251	1251	1261	1267
UC-15	1.0	67.9	0.324	1341	1465	1507	1507	1549	1558
UC-16	1.0	67.2	0.332	1991	2109	2139	2139	2195	2195
UC-22	1.0	68.8	0.319	1187	1187	1187	1187	1187	1187
UC-23	1.0	68.4	0.323	1333	1343	1349	1349	1357	1357
UC-24	1.0	67.0	0.337	1991	2165	2269	2269	2401	2405
UC-30	1.0	67.3	0.332	1729	1899	1969	1969	2033	2055
UC-31	1.0	66.8	0.337	2001	2211	2325	2325	2563	2576
UC-32	1.0	68.0	0.326	1583	1595	1603	1603	1619	1620
UC-38	1.0	67.3	0.333	1915	2001	2029	2029	2079	2083
UC-39	1.0	66.8	0.336	2089	2317	2427	2427	2519	2540
UC-40	1.0	65.7	0.348	2275	2457	2565	2565	2679	2679
UC-6	1.0	68.0	0.325	1639	1795	1813	1813	1821	1821
UC-7	1.0	68.0	0.324	1247	1249	1251	1251	1251	1252
UC-8	1.0	66.0	0.343	2185	2393	2513	2513	2705	2764

Table A-6: 4.3.4.2 Low-Cycle Population Tests, HG1 Coupons, Random Grain Orientation

Test	Strain Amp. (%)	Stress Amp. (Ksi)	Plastic Strain Amp. (%)	Peak Load Drop Failure Life ($2N_f$)					
				2%	5%	10%	25%	50%	Fracture
LP3-6	1.2	68.3	0.511	1282	1352	1404	1436	1450	1450
LP3-15	1.2	67.3	0.528	1264	1376	1436	1506	1550	1598
LP3-24	1.2	69.3	0.510	922	1024	1034	1040	1040	1040
LP3-1	1.2	69.6	0.507	792	800	806	810	812	812
LP3-17	1.2	68.3	0.520	1020	1074	1106	1144	1154	1154
LP3-31	1.2	69.7	0.506	824	858	870	878	882	886
LP3-41	1.2	68.8	0.516	880	922	942	970	980	980
LP3-50	1.2	68.3	0.520	1124	1194	1228	1252	1264	1270
LP3-38	1.2	68.2	0.523	1204	1298	1340	1378	1400	1416
LP3-29	1.2	68.2	0.524	1110	1170	1198	1222	1234	1234
LP3-8	1.5	70.0	0.795	844	920	948	976	988	994
LP3-13	1.5	71.4	0.788	504	556	562	568	570	570
LP3-4	1.5	73.1	0.772	468	504	514	518	522	522
LP3-36	1.5	69.5	0.809	838	928	956	968	972	972
LP3-18	1.5	71.6	0.788	548	590	606	624	632	632
LP3-28	1.5	72.7	0.777	488	508	514	520	524	524
LP3-47	1.5	69.9	0.806	778	856	872	888	896	898
LP3-35	1.5	71.7	0.788	582	612	624	632	638	642
LP3-42	1.5	68.8	0.817	840	922	956	986	1006	1010
LP3-25	1.5	74.1	0.764	462	464	466	470	472	472
LP3-34	2.0	73.3	1.27	408	450	462	470	472	472
LP3-39	2.0	77.5	1.23	246	246	248	248	248	248
LP3-21	2.0	73.0	1.27	402	432	438	440	440	440
LP3-19	2.0	77.8	1.23	260	262	264	264	264	264
LP3-43	2.0	77.4	1.23	282	290	292	292	292	292
LP3-49	2.0	76.3	1.24	296	338	340	342	342	342
LP3-26	2.0	73.1	1.28	446	484	498	508	512	512
LP3-12	2.0	73.5	1.27	386	412	418	422	422	422
LP3-5	2.0	74.1	1.27	326	374	382	386	386	386
LP3-10	2.0	72.6	1.29	444	482	486	492	500	504
LP3-7	3.0	81.8	2.19	126	128	130	130	130	130
LP3-30	3.0	81.6	2.19	138	140	142	142	142	142
LP3-2	3.0	81.3	2.19	132	134	136	136	136	136
LP3-33	3.0	78.9	2.22	178	192	194	196	196	196
LP3-22	3.0	82.9	2.18	112	112	114	114	114	114
LP3-20	3.0	77.2	2.23	206	228	230	234	234	236
LP3-45	3.0	82.0	2.19	126	128	130	130	130	130
LP3-14	3.0	76.9	2.24	192	246	248	252	252	252
LP3-37	3.0	80.7	2.20	134	138	140	140	140	140
LP3-11	4.0	80.6	3.19	134	142	142	142	142	142
LP3-9	4.0	81.7	3.18	108	118	120	120	120	120
LP3-3	4.0	85.7	3.15	74	74	74	74	74	74
LP3-32	4.0	79.9	3.20	126	134	136	136	136	136
LP3-40	4.0	80.7	3.20	110	116	118	120	120	120
LP3-48	4.0	79.4	3.21	134	154	156	156	156	156
LP3-27	4.0	82.2	3.18	96	98	98	98	98	98
LP3-23	4.0	84.7	3.16	76	78	78	78	78	78
LP3-16	4.0	81.3	3.19	118	128	130	130	130	130
LP3-44	4.0	83.4	3.17	86	88	90	90	90	90

Table A-7: 4.3.4.2 Intermediate-Cycle Population Tests, HG1 Coupons, Random Grain Orientation

Test	Strain Amp. (%)	Stress Amp. (Ksi)	Plastic Strain Amp. (%)	Peak Load Drop Failure Life ($2N_f$)					
				2%	5%	10%	25%	50%	Fracture
IP1-10	0.6	59.7	0.00578	6982	7536	7824	8336	8834	9804
IP1-11	0.6	59.4	0.00833	7462	8494	8542	8646	8764	8924
IP1-14	0.6	59.7	0.00689	9354	9552	9680	9844	9936	9946
IP1-16	0.6	60.1	0.00325	9774	9906	10022	10116	10290	10356
IP1-18	0.6	59.8	0.00440	10578	10646	10726	10890	11100	11103
IP1-2	0.6	59.2	0.0168	10248	10314	10366	10438	10540	10558
IP1-20	0.6	62.5	0.00148	6878	7236	7498	7750	7834	7844
IP1-3	0.6	60.6	0.00325	7986	8460	8760	9088	9140	9150
IP1-5	0.6	60.2	0.00301	5460	5888	6172	6622	6968	6972
IP1-8	0.6	61.1	0.00427	9048	9166	9218	9268	9284	9284
IP1-1	0.7	65.5	0.0501	3390	3472	3526	3576	3582	3586
IP1-12	0.7	64.1	0.0624	4236	4758	5038	5320	5504	5528
IP1-13	0.7	65.1	0.0528	3408	3788	3848	3892	3908	3908
IP1-15	0.7	65.2	0.0527	3602	3944	4126	4326	4362	4388
IP1-17	0.7	65.8	0.0469	2756	2758	2758	2758	2758	2758
IP1-19	0.7	64.5	0.0584	4104	4694	4768	4850	4920	5008
IP1-4	0.7	64.6	0.0637	3998	4180	4252	4332	4398	4446
IP1-6	0.7	64.8	0.0560	4092	4182	4222	4328	4350	4350
IP1-7	0.7	66.1	0.0427	2938	2958	2976	2992	3020	3027
IP1-9	0.7	65.1	0.0530	3892	4110	4176	4206	4214	4214

Table A-8: 4.3.4.2 Intermediate-Cycle Population Tests, HG1 Coupons, Controlled Grain Orientation

Test	Strain Amp. (%)	Stress Amp. (Ksi)	Plastic Strain Amp. (%)	Peak Load Drop Failure Life ($2N_f$)					
				2%	5%	10%	25%	50%	Fracture
IPG1-10	0.6	59.3	0.0145	9242	9474	9712	10032	10072	10072
IPG1-2	0.6	59.5	0.0144	8624	9150	9322	9526	9706	9798
IPG1-3	0.6	59.5	0.0131	9860	10212	10362	10480	10530	10568
IPG1-5	0.6	59.2	0.0162	8610	8648	8704	8812	8842	8844
IPG1-8	0.6	59.1	0.0168	8598	9464	9848	10276	10538	10552
IPG1-1	0.7	64.4	0.0646	4542	4950	5174	5496	5528	5528
IPG1-4	0.7	63.8	0.0713	4246	4646	4862	5124	5344	5472
IPG1-6	0.7	64.2	0.0682	4510	5012	5264	5586	5886	5886
IPG1-7	0.7	64.5	0.0639	4228	4696	4834	4978	5076	5114
IPG1-9	0.7	64.3	0.0651	4420	4902	5128	5372	5444	5444

Table A-9: 4.3.4.2 Low-Cycle Population Tests, HG1 Coupons, Controlled Grain Orientation

Test	Strain Amp. (%)	Stress Amp. (Ksi)	Plastic Strain Amp. (%)	Peak Load Drop Failure Life ($2N_f$)					
				2%	5%	10%	25%	50%	Fracture
LPG1-12	1.2	67.1	0.537	1196	1286	1342	1402	1432	1442
LPG1-16	1.2	68.2	0.528	1326	1438	1506	1592	1656	1664
LPG1-25	1.2	67.6	0.536	1336	1424	1466	1516	1560	1584
LPG1-3	1.2	68.1	0.530	1296	1450	1518	1552	1564	1566
LPG1-9	1.2	67.8	0.532	1502	1546	1612	1690	1720	1728
LPG1-14	1.5	69.1	0.817	864	948	978	1016	1046	1048
LPG1-19	1.5	69.5	0.816	870	930	964	998	1012	1030
LPG1-21	1.5	69.6	0.816	812	896	932	968	984	996
LPG1-5	1.5	69.5	0.815	856	948	990	1038	1044	1048
LPG1-6	1.5	70.0	0.806	796	874	908	944	960	960
LPG1-10	2.0	72.8	1.29	492	542	556	570	576	576
LPG1-13	2.0	72.7	1.28	504	542	566	582	584	584
LPG1-2	2.0	72.7	1.28	484	506	522	528	530	534
LPG1-20	2.0	72.7	1.28	512	582	598	604	604	604
LPG1-24	2.0	72.6	1.28	478	512	524	534	542	544
LPG1-1	3.0	76.7	2.25	210	226	230	232	232	232
LPG1-15	3.0	77.2	2.24	220	234	236	240	240	240
LPG1-18	3.0	77.2	2.23	206	220	222	222	224	224
LPG1-22	3.0	77.3	2.24	172	182	186	188	190	190
LPG1-8	3.0	77.3	2.24	210	214	216	218	218	218
LPG1-11	4.0	80.5	3.21	126	140	142	142	142	142
LPG1-17	4.0	81.2	3.20	122	134	136	138	138	138
LPG1-23	4.0	80.4	3.20	116	130	132	134	134	134
LPG1-4	4.0	81.4	3.20	124	136	140	140	140	140
LPG1-7	4.0	80.8	3.20	120	130	132	132	132	132

Table A-10: 4.3.4.2 Additional Low-Cycle Population Tests, HG1 Coupons, Controlled Grain Orientation

Test	Strain Amp. (%)	Stress Amp. (Ksi)	Plastic Strain Amp. (%)	Peak Load Drop Failure Life ($2N_f$)					
				2%	5%	10%	25%	50%	Fracture
LPGA1-1	0.8	65.2	0.152	3374	3576	3742	3926	3998	4090
LPGA1-3	0.8	65.1	0.155	3356	3762	4030	4204	4284	4332
LPGA1-5	0.8	65.3	0.152	3404	3692	3866	4094	4164	4164
LPGA1-7	0.8	66.1	0.144	3120	3498	3640	3734	3776	3876
LPGA1-9	0.8	65.1	0.153	3334	3626	3802	4018	4130	4278
LPGA1-10	1.0	67.2	0.333	2042	2238	2340	2458	2524	2574
LPGA1-2	1.0	66.6	0.338	2058	2216	2304	2408	2486	2486
LPGA1-4	1.0	66.9	0.335	1934	2104	2230	2392	2456	2479
LPAG1-6	1.0	67.4	0.330	2198	2428	2550	2686	2714	2728
LPGA1-8	1.0	67.4	0.331	1452	1628	1730	1852	1906	1956

Table A-11: Metcut Low-Cycle Population Tests, HG1 Coupons, Controlled Grain Orientation

Test	Strain Amp. (%)	Stress Amp. (Ksi)	Plastic Strain Amp. (%)	Peak Load Drop Failure Life ($2N_f$)					
				2%	5%	10%	25%	50%	Fracture
LPG2-11	1.2	67.2	0.529	1485	1561	1615	1691	1755	1785
LPG2-18	1.2	67.3	0.529	1569	1695	1751	1793	1809	1810
LPG2-21	1.2	67.2	0.535	1587	1737	1803	1873	1925	1925
LPG2-29	1.2	67.2	0.534	1471	1597	1653	1727	1773	1795
LPG2-3	1.2	67.7	0.531	1361	1453	1503	1549	1587	1616
LPG2-33	1.2	67.4	0.532	1521	1669	1749	1823	1857	1860
LPG2-37	1.2	66.3	0.542	1643	1795	1873	1981	2035	2062
LPG2-42	1.2	68.1	0.526	1295	1397	1455	1517	1521	1521
LPG2-50	1.2	67.8	0.530	1581	1739	1801	1857	1897	1897
LPG2-52	1.2	67.3	0.533	1501	1613	1681	1769	1823	1831
LPG2-57	1.2	67.8	0.530	1517	1633	1685	1753	1791	1825
LPG2-65	1.2	67.2	0.532	1687	1811	1893	1969	2029	2029
LPG2-66	1.2	67.6	0.529	1573	1685	1737	1813	1859	1859
LPG2-75	1.2	67.1	0.535	1423	1519	1557	1609	1635	1660
LPG2-9	1.2	67.6	0.529	1489	1585	1641	1705	1741	1762
LPG2-13	1.5	69.0	0.815	1059	1139	1173	1205	1223	1228
LPG2-19	1.5	68.5	0.818	1047	1135	1177	1221	1239	1244
LPG2-2	1.5	69.3	0.815	925	1003	1037	1061	1091	1091
LPG2-24	1.5	69.0	0.817	1005	1097	1139	1205	1231	1234
LPG2-26	1.5	68.6	0.819	869	931	969	1013	1027	1040
LPG2-35	1.5	69.1	0.816	975	1045	1081	1121	1163	1165
LPG2-40	1.5	68.6	0.820	997	1073	1113	1147	1165	1171
LPG2-45	1.5	69.0	0.816	899	981	1019	1051	1069	1073
LPG2-49	1.5	69.0	0.816	977	1069	1105	1135	1155	1161
LPG2-55	1.5	69.2	0.815	1067	1183	1225	1277	1311	1313
LPG2-59	1.5	69.3	0.813	1089	1199	1233	1277	1301	1306
LPG2-6	1.5	68.7	0.819	977	1071	1105	1137	1137	1138
LPG2-61	1.5	68.9	0.817	1023	1121	1159	1195	1203	1203
LPG2-69	1.5	69.2	0.814	1043	1113	1155	1193	1209	1217
LPG2-73	1.5	68.3	0.823	899	971	1009	1059	1083	1089
LPG2-15	2.0	71.7	1.29	585	631	649	663	665	666
LPG2-17	2.0	72.1	1.29	537	587	609	627	627	627
LPG2-25	2.0	70.9	1.30	561	589	605	619	627	628
LPG2-30	2.0	71.4	1.29	559	601	617	623	625	626
LPG2-32	2.0	71.2	1.29	593	639	651	659	663	663
LPG2-39	2.0	71.7	1.29	571	629	645	661	667	667
LPG2-41	2.0	71.6	1.29	577	611	621	637	645	646
LPG2-48	2.0	71.3	1.29	525	567	577	599	609	610
LPG2-5	2.0	71.8	1.29	483	571	585	593	599	600
LPG2-51	2.0	72.2	1.29	575	619	633	643	647	648
LPG2-58	2.0	71.1	1.29	589	625	639	653	661	665
LPG2-63	2.0	71.6	1.29	595	643	659	669	669	670
LPG2-70	2.0	71.6	1.29	579	623	637	657	663	663
LPG2-71	2.0	71.4	1.29	557	597	609	615	617	619
LPG2-8	2.0	71.1	1.30	585	637	659	669	673	674
LPG2-10	3.0	76.4	2.24	239	269	273	275	275	276
LPG2-12	3.0	76.2	2.24	246	282	286	286	286	286
LPG2-20	3.0	76.8	2.24	239	261	269	275	275	276

Table A-11: (Cont'd)

Test	Strain Amp. (%)	Stress Amp. (Ksi)	Plastic Strain Amp. (%)	Peak Load Drop Failure Life ($2N_f$)					
				2%	5%	10%	25%	50%	Fracture
LPG2-23	3.0	76.2	2.25	233	251	257	259	259	260
LPG2-27	3.0	76.2	2.24	261	293	295	295	295	296
LPG2-31	3.0	76.4	2.24	237	277	287	289	289	290
LPG2-36	3.0	75.9	2.25	241	273	275	275	275	276
LPG2-4	3.0	77.2	2.24	223	231	235	237	241	242
LPG2-44	3.0	76.5	2.24	239	277	285	285	285	286
LPG2-46	3.0	76.3	2.24	241	267	271	273	273	274
LPG2-60	3.0	76.1	2.24	231	247	253	255	257	257
LPG2-64	3.0	75.6	2.25	239	259	263	267	267	268
LPG2-68	3.0	76.9	2.24	243	257	261	263	263	263
LPG2-74	3.0	76.5	2.24	245	265	271	275	275	276
LPG2-1	4.0	79.8	3.21	133	147	149	151	151	152
LPG2-14	4.0	79.5	3.20	143	165	167	167	167	168
LPG2-16	4.0	79.4	3.21	139	151	153	153	153	154
LPG2-22	4.0	78.8	3.22	131	139	141	141	141	142
LPG2-28	4.0	79.7	3.21	137	151	153	153	153	154
LPG2-34	4.0	79.3	3.21	141	157	161	161	161	162
LPG2-38	4.0	79.2	3.21	137	151	153	153	153	154
LPG2-43	4.0	79.4	3.21	143	151	155	155	155	155
LPG2-47	4.0	80.0	3.21	137	157	161	161	161	161
LPG2-53	4.0	80.0	3.21	143	165	167	167	167	168
LPG2-56	4.0	79.1	3.22	135	147	149	149	149	150
LPG2-62	4.0	79.4	3.21	139	151	155	155	155	156
LPG2-67	4.0	80.0	3.21	135	153	155	155	155	155
LPG2-7	4.0	79.3	3.21	137	153	155	155	155	156
LPG2-72	4.0	79.7	3.21	141	153	155	155	155	155

Table A-12: Metcut Additional Low-Cycle Population Tests, HG1 Coupons, Controlled Grain Orientation

Test	Strain Amp. (%)	Stress Amp. (Ksi)	Plastic Strain Amp. (%)	Peak Load Drop Failure Life ($2N_f$)					
				2%	5%	10%	25%	50%	Fracture
LPGA2-1	0.8	65.0	0.155	3079	3397	3597	3743	3791	3806
LPGA2-10	0.8	65.2	0.153	3879	4163	4233	4259	4287	4303
LPGA2-11	0.8	64.9	0.156	3695	4071	4281	4465	4479	4479
LPGA2-13	0.8	64.6	0.160	3485	3883	4117	4367	4391	4392
LPGA2-16	0.8	64.9	0.155	3651	4059	4277	4605	4813	4829
LPGA2-17	0.8	65.0	0.156	3549	3891	4023	4195	4313	4313
LPGA2-19	0.8	65.2	0.159	4003	4211	4497	4705	4769	4769
LPGA2-23	0.8	65.1	0.159	3693	3889	4055	4263	4449	4481
LPGA2-25	0.8	65.3	0.158	4003	4283	4511	4735	4829	4835
LPGA2-27	0.8	64.9	0.160	3763	4069	4245	4467	4575	4695
LPGA2-29	0.8	65.1	0.160	3687	4149	4379	4535	4623	4623
LPGA2-3	0.8	64.4	0.162	2443	2687	2813	2949	3035	3134
LPGA2-5	0.8	64.8	0.158	2875	3189	3371	3625	3805	4002
LPGA2-8	0.8	65.1	0.156	3337	3675	3927	3969	3969	3970
LPGA2-12	1.0	67.0	0.337	2299	2483	2573	2703	2807	2884
LPGA2-14	1.0	66.3	0.342	2037	2197	2291	2411	2475	2475
LPGA2-15	1.0	66.5	0.348	2115	2325	2443	2581	2619	2619
LPGA2-18	1.0	66.5	0.349	2001	2175	2271	2385	2469	2512
LPGA2-2	1.0	66.5	0.342	2387	2599	2737	2901	2945	2945
LPGA2-20	1.0	67.1	0.345	2109	2313	2413	2553	2635	2635
LPGA2-21	1.0	66.4	0.349	2179	2397	2505	2643	2749	2749
LPGA2-24	1.0	66.4	0.351	2059	2215	2331	2511	2669	2682
LPGA2-26	1.0	66.8	0.346	2183	2351	2445	2501	2515	2515
LPGA2-28	1.0	66.7	0.347	2195	2409	2503	2615	2639	2639
LPGA2-30	1.0	66.7	0.349	1827	1977	2087	2237	2373	2391
LPGA2-4	1.0	66.1	0.345	1983	2159	2247	2335	2397	2462
LPGA2-6	1.0	67.0	0.334	2289	2463	2567	2669	2721	2721
LPGA2-7	1.0	66.9	0.338	2201	2409	2507	2591	2619	2639
LPGA2-9	1.0	65.9	0.349	2319	2481	2589	2697	2731	2750

Table A-13: Metcut Intermediate-Cycle Population Tests, HG1 Coupons, Controlled Grain Orientation

Test	Strain Amp. (%)	Stress Amp. (Ksi)	Plastic Strain Amp. (%)	Peak Load Drop Failure Life ($2N_f$)					
				2%	5%	10%	25%	50%	Fracture
IPG2-10	0.6	57.7	0.0292	12729	13147	13359	13619	13755	13922
IPG2-11	0.6	57.4	0.0314	11921	12295	12497	12695	12867	13084
IPG2-14	0.6	57.7	0.0304	13553	13761	13989	14291	14315	14315
IPG2-15	0.6	57.5	0.0315	12547	12565	12599	12665	12721	12859
IPG2-17	0.6	57.8	0.0297	9045	9093	9159	9305	9483	9563
IPG2-2	0.6	57.5	0.0307	11387	11639	11973	12425	12451	12472
IPG2-20	0.6	57.9	0.0249	13257	13403	13569	13989	14073	14085
IPG2-22	0.6	56.9	0.0343	11391	12253	12655	13169	13391	13401
IPG2-24	0.6	57.6	0.0302	12875	13233	13457	13659	13875	14074
IPG2-25	0.6	57.3	0.0330	12871	13437	13857	14289	14907	14907
IPG2-27	0.6	57.4	0.0310	10649	10727	10809	10959	11091	11311
IPG2-29	0.6	57.1	0.0346	11231	11281	11335	11497	11673	11885
IPG2-3	0.6	57.9	0.0220	12203	13009	13169	13317	13449	13701
IPG2-6	0.6	57.6	0.0276	13211	13265	13337	13433	13517	13647
IPG2-8	0.6	58.4	0.0203	11811	12083	12305	12659	12841	12843
IPG2-1	0.7	63.3	0.0710	4277	4673	5001	5387	5759	6051
IPG2-12	0.7	63.5	0.0727	6217	6487	6665	6971	7133	7204
IPG2-13	0.7	63.2	0.0767	5775	6247	6413	6513	6581	6593
IPG2-16	0.7	63.6	0.0731	5357	5841	6015	6125	6285	6484
IPG2-18	0.7	63.0	0.0756	5511	5733	5923	6217	6629	6691
IPG2-19	0.7	63.2	0.0707	5465	5969	6309	6601	6699	6739
IPG2-21	0.7	63.1	0.0722	5669	6023	6213	6467	6761	6765
IPG2-23	0.7	63.3	0.0703	5785	6447	6719	6925	7073	7249
IPG2-26	0.7	63.7	0.0687	5413	5807	6035	6349	6673	6804
IPG2-28	0.7	63.0	0.0733	6631	6867	6961	7077	7183	7319
IPG2-30	0.7	63.5	0.0723	5345	5879	6379	6473	6499	6500
IPG2-4	0.7	63.3	0.0746	4843	5267	5569	5629	5685	5717
IPG2-5	0.7	62.7	0.0787	5757	6099	6291	6547	6687	6703
IPG2-7	0.7	62.7	0.0758	5793	6171	6373	6737	7079	7118
IPG2-9	0.7	63.4	0.0739	6327	6835	7011	7187	7235	7235

Table A-14: Metcut Low-Cycle Population Tests, UG3 Coupons

Test	Strain Amp. (%)	Stress Amp. (Ksi)	Plastic Strain Amp. (%)	Peak Load Drop Failure Life ($2N_f$)					
				2%	5%	10%	25%	50%	Fracture
LPUG-14	0.8	65.8	0.147	2915	3085	3181	3299	3407	3544
LPUG-22	0.8	65.2	0.156	2167	2255	2331	2375	2379	2379
LPUG-34	0.8	64.3	0.164	2191	2253	2295	2345	2357	2357
LPUG-46	0.8	64.9	0.157	2891	3029	3109	3253	3393	3393
LPUG-20	1.0	65.6	0.351	949	1005	1049	1139	1267	1340
LPUG-27	1.0	65.9	0.342	1179	1241	1283	1341	1379	1380
LPUG-32	1.0	65.6	0.347	1151	1221	1271	1377	1441	1442
LPUG-38	1.0	66.3	0.339	1215	1253	1275	1311	1345	1358
LPUG-6	1.0	66.1	0.344	1001	1025	1043	1083	1159	1176
LPUG-12	1.2	66.8	0.536	615	641	661	691	731	742
LPUG-17	1.2	67.5	0.532	575	585	595	611	615	615
LPUG-30	1.2	68.1	0.524	501	521	535	569	619	638
LPUG-8	1.2	67.6	0.520	557	585	599	609	617	620
LPUG-29	1.5	68.9	0.814	321	395	401	405	411	412
LPUG-31	1.5	69.6	0.802	389	403	411	427	435	435
LPUG-39	1.5	68.9	0.812	333	361	365	381	389	390
LPUG-33	2.0	70.2	1.30	203	215	225	259	271	271
LPUG-7	2.0	70.5	1.28	178	222	230	234	234	234

Table A-15: Metcut Intermediate-Cycle Population Tests, UG3 Coupons

Test	Strain Amp. (%)	Stress Amp. (Ksi)	Plastic Strain Amp. (%)	Peak Load Drop Failure Life ($2N_f$)					
				2%	5%	10%	25%	50%	Fracture
IPUG-10	0.6	61.0	1e-006	8479	8537	8605	8677	8697	8751
IPUG-9	0.6	64.6	0.0608	3307	3585	3693	3869	3953	3953
IPUG-1	0.7	64.2	0.0638	3679	3755	3805	3867	3907	3956
IPUG-12	0.7	64.3	0.0652	3881	4197	4393	4709	5035	5161
IPUG-13	0.7	64.0	0.0670	3759	3821	3855	3901	3931	3953
IPUG-16	0.7	64.1	0.0647	3945	4153	4239	4375	4483	4483
IPUG-17	0.7	65.1	0.0562	3869	4077	4159	4217	4235	4237
IPUG-20	0.7	64.4	0.0623	3003	3003	3179	3495	3867	3867
IPUG-5	0.7	64.3	0.0647	3643	3717	3773	3837	3883	3888
IPUG-7	0.7	65.3	0.0602	3107	3283	3403	3649	4049	4429

Table A-16: 4.3.4.2 High-Cycle Population Tests, HG1 Coupons

Test	Strain Amp. (%)	Failure ($2N_f$)	Runout ($2N_f$)	Test	Strain Amp. (%)	Failure ($2N_f$)	Runout ($2N_f$)
HP1-12	0.5	30126		HP1-11	0.3	2.6456e+05	
HP1-14	0.5	28130		HP1-13	0.3	3.3135e+05	
HP1-17	0.5	28872		HP1-18	0.3	2.6411e+05	
HP1-21	0.5	28314		HP1-22	0.3	2.9562e+05	
HP1-25	0.5	26134		HP1-28	0.3	2.7937e+05	
HP1-29	0.5	27718		HP1-32	0.3	2.6187e+05	
HP1-3	0.5	28648		HP1-35	0.3	3.0708e+05	
HP1-33	0.5	26568		HP1-39	0.3	2.5612e+05	
HP1-40	0.5	30764		HP1-44	0.3	3.5135e+05	
HP1-41	0.5	29468		HP1-47	0.3	3.2996e+05	
HP1-45	0.5	25246		HP1-49	0.3	3.416e+05	
HP1-52	0.5	29900		HP1-54	0.3	3.0311e+05	
HP1-56	0.5	26420		HP1-60	0.3	2.9163e+05	
HP1-57	0.5	27606		HP1-8	0.3	1.913e+05	
HP1-6	0.5	26842		HP1-23	0.25	6.657e+05	
HP1-15	0.4	68974		HP1-27	0.25	5.9717e+05	
HP1-19	0.4	89232		HP1-30	0.25	7.3899e+05	
HP1-2	0.4	83578		HP1-34	0.25	8.9588e+05	
HP1-24	0.4	84962		HP1-37	0.25	8.3254e+05	
HP1-26	0.4	75256		HP1-42	0.25	6.526e+05	
HP1-31	0.4	81280		HP1-48	0.25	6.6088e+05	
HP1-36	0.4	87984		HP1-51	0.25	6.0975e+05	
HP1-38	0.4	85514		HP1-55	0.25	6.864e+05	
HP1-43	0.4	66852		HP1-59	0.25	7.6273e+05	
HP1-46	0.4	88486		HP1-61	0.22	1.3701e+06	
HP1-50	0.4	84188		HP1-10	0.2	2.0494e+07	√
HP1-53	0.4	71308		HP1-16	0.2	2.4658e+07	√
HP1-58	0.4	95990		HP1-20	0.2	2.0167e+07	√
HP1-7	0.4	69706		HP1-4	0.2	2.0468e+07	√
HP1-9	0.4	88604		HP1-5	0.2	2.0154e+07	√
HP1-1	0.3	2.9118e+05					

Table A-17: Metcut High-Cycle Population Tests, HG1 Coupons

Test	Strain Amp. (%)	Failure ($2N_f$)	Runout ($2N_f$)	Test	Strain Amp. (%)	Failure ($2N_f$)	Runout ($2N_f$)
HP2-13	0.5	27492		HP2-8	0.4	72196	
HP2-17	0.5	31582		HP2-1	0.3	4.6824e+05	
HP2-24	0.5	32710		HP2-16	0.3	4.6516e+05	
HP2-28	0.5	29936		HP2-19	0.3	7.3211e+05	
HP2-29	0.5	30644		HP2-23	0.3	3.4307e+05	
HP2-34	0.5	32714		HP2-27	0.3	3.8281e+05	
HP2-38	0.5	28984		HP2-31	0.3	3.1671e+05	
HP2-4	0.5	27484		HP2-36	0.3	3.7935e+05	
HP2-41	0.5	31558		HP2-37	0.3	2.9518e+05	
HP2-45	0.5	32226		HP2-44	0.3	5.3782e+05	
HP2-5	0.5	37500		HP2-46	0.3	3.0894e+05	
HP2-52	0.5	32804		HP2-50	0.3	5.4353e+05	
HP2-55	0.5	26908		HP2-53	0.3	5.7377e+05	
HP2-57	0.5	32090		HP2-6	0.3	3.9962e+05	
HP2-9	0.5	28848		HP2-60	0.3	8.4755e+05	
HP2-10	0.4	83320		HP2-21	0.27	1.1773e+07	
HP2-15	0.4	71042		HP2-26	0.27	2.4803e+06	
HP2-2	0.4	71672		HP2-33	0.27	5.6586e+06	
HP2-20	0.4	72386		HP2-40	0.27	1.3618e+06	
HP2-22	0.4	79338		HP2-43	0.27	7.8531e+06	
HP2-25	0.4	76892		HP2-48	0.27	4.165e+06	
HP2-30	0.4	62018		HP2-51	0.27	8.5724e+05	
HP2-35	0.4	68390		HP2-56	0.27	1.7101e+06	
HP2-39	0.4	72872		HP2-58	0.27	9.1351e+06	
HP2-42	0.4	97864		HP2-32	0.27	2.0065e+07	√
HP2-47	0.4	88850		HP2-11	0.25	2.5512e+07	√
HP2-49	0.4	83472		HP2-14	0.25	2.012e+07	√
HP2-54	0.4	88184		HP2-18	0.25	3.5313e+07	√
HP2-59	0.4	76828					

Table A-18: Metcut High-Cycle Population Tests, UG3 Coupons

Test	Strain Amp. (%)	Failure ($2N_f$)	Runout ($2N_f$)	Test	Strain Amp. (%)	Failure ($2N_f$)	Runout ($2N_f$)
HPUG-15	0.5	30754		HPUG-26	0.3	4.8485e+05	
HPUG-20	0.5	32432		HPUG-34	0.3	1.747e+06	
HPUG-22	0.5	21642		HPUG-4	0.3	5.5272e+05	
HPUG-31	0.5	35344		HPUG-40	0.3	2.5275e+06	
HPUG-35	0.5	32092		HPUG-44	0.3	5.1028e+05	
HPUG-38	0.5	28936		HPUG-45	0.3	6.8461e+05	
HPUG-41	0.5	31658		HPUG-49	0.3	5.5832e+05	
HPUG-46	0.5	27148		HPUG-57	0.3	9.9055e+05	
HPUG-50	0.5	31690		HPUG-8	0.3	2.8003e+05	
HPUG-53	0.5	31056		HPUG-1	0.25	2.6818e+05	
HPUG-59	0.5	25238		HPUG-11	0.25	1.6075e+07	
HPUG-6	0.5	37500		HPUG-14	0.25	2.8294e+07	
HPUG-12	0.4	1.0194e+05		HPUG-24	0.25	1.2107e+07	
HPUG-16	0.4	87536		HPUG-48	0.25	2.6805e+05	
HPUG-21	0.4	72700		HPUG-7	0.25	1.5022e+06	
HPUG-28	0.4	80514		HPUG-19	0.25	4.0924e+07	√
HPUG-36	0.4	78652		HPUG-27	0.25	2.0228e+07	√
HPUG-37	0.4	94276		HPUG-30	0.25	2.0044e+07	√
HPUG-47	0.4	80770		HPUG-39	0.25	2.351e+07	√
HPUG-5	0.4	99942		HPUG-43	0.25	2.0395e+07	√
HPUG-56	0.4	85378		HPUG-51	0.25	2.0078e+07	√
HPUG-13	0.3	3.2734e+05		HPUG-55	0.25	2.0045e+07	√
HPUG-17	0.3	3.0131e+05		HPUG-60	0.25	2.0105e+07	√
HPUG-23	0.3	5.4644e+05					

APPENDIX B
HYSTERESIS LOOP PLOTS

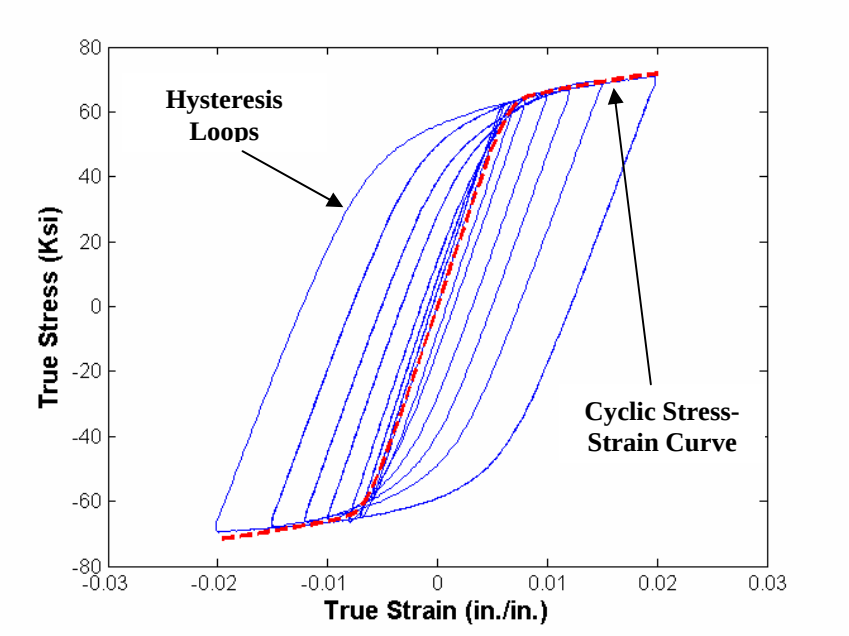

Figure B-1: Cyclic Stress-Strain Curve Comparison with UG3 Coupon Stabilized Hysteresis Loops

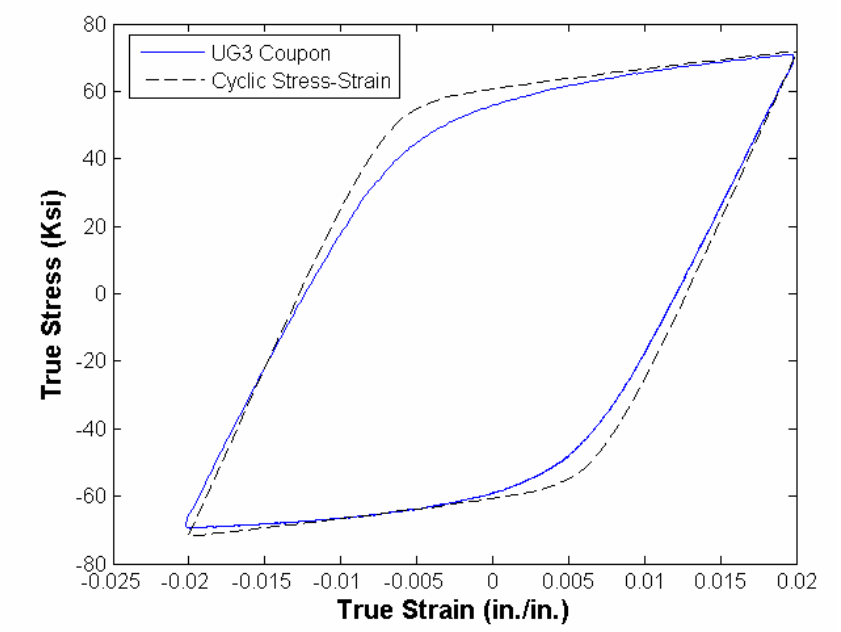

Figure B-2: Massing Hysteresis Loop Comparison with UG3 Coupon Stabilized 2.0% Strain Hysteresis Loop

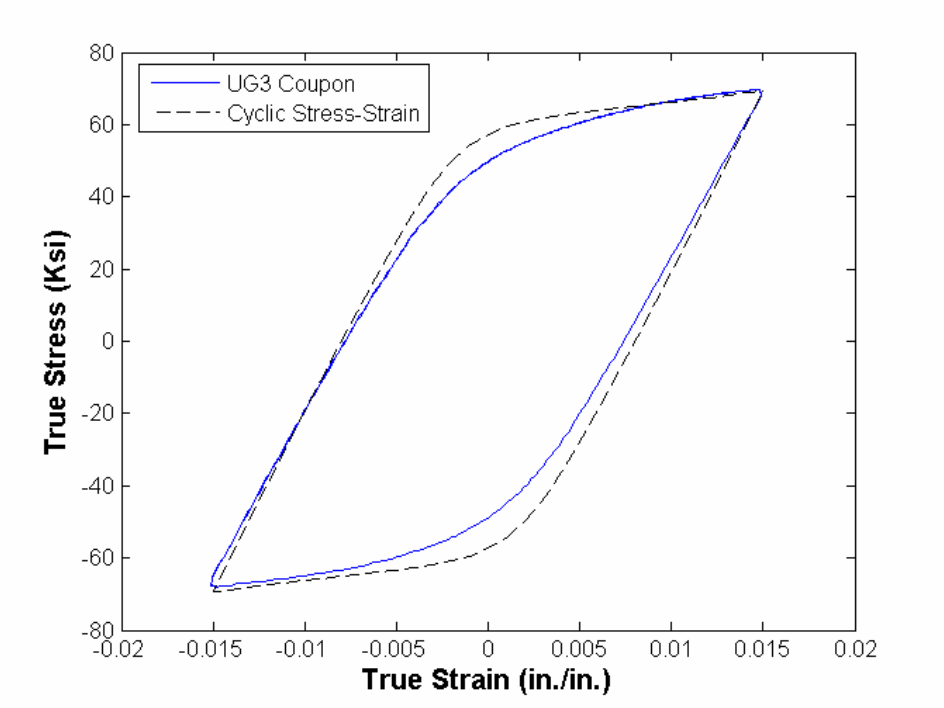

Figure B-3: Massing Hysteresis Loop Comparison with UG3 Coupon Stabilized 1.5% Strain Hysteresis Loop

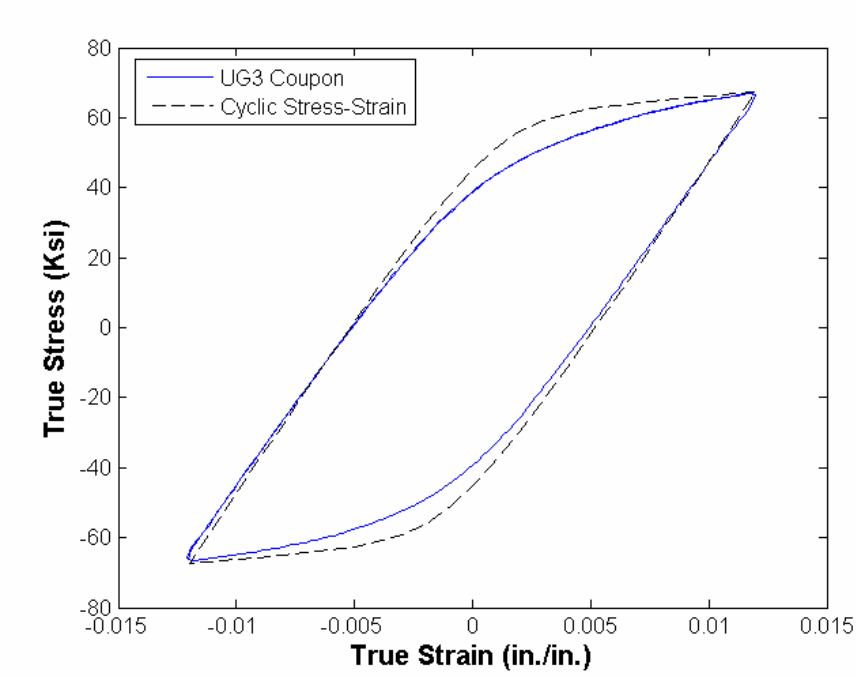

Figure B-4: Massing Hysteresis Loop Comparison with UG3 Coupon Stabilized 1.2% Strain Hysteresis Loop

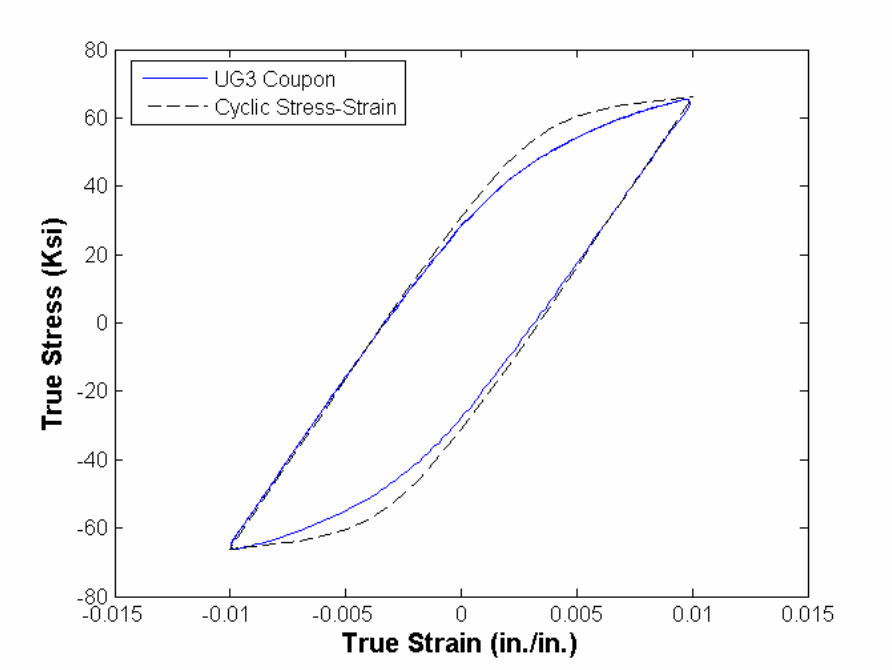

Figure B-5: Massing Hysteresis Loop Comparison with UG3 Coupon Stabilized 1.0% Strain Hysteresis Loop

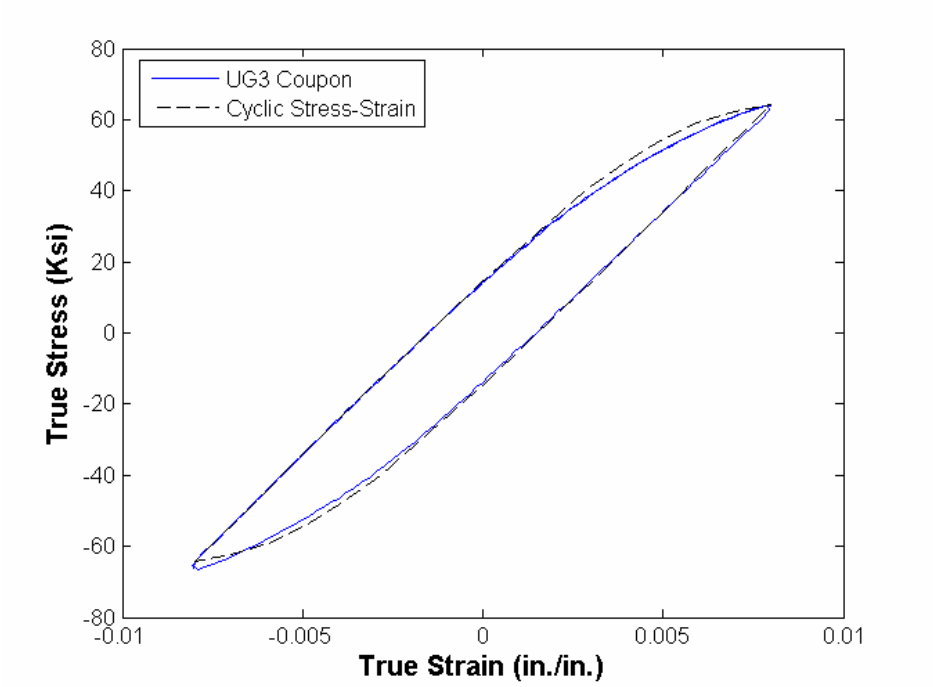

Figure B-6: Massing Hysteresis Loop Comparison with UG3 Coupon Stabilized 0.8% Strain Hysteresis Loop

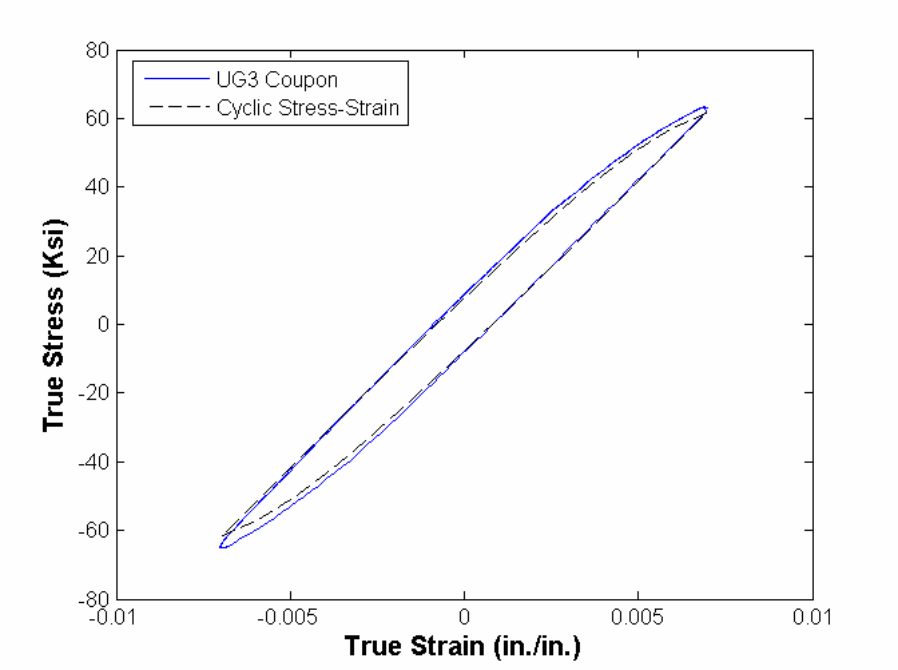

Figure B-7: Massing Hysteresis Loop Comparison with UG3 Coupon Stabilized 0.7% Strain Hysteresis Loop

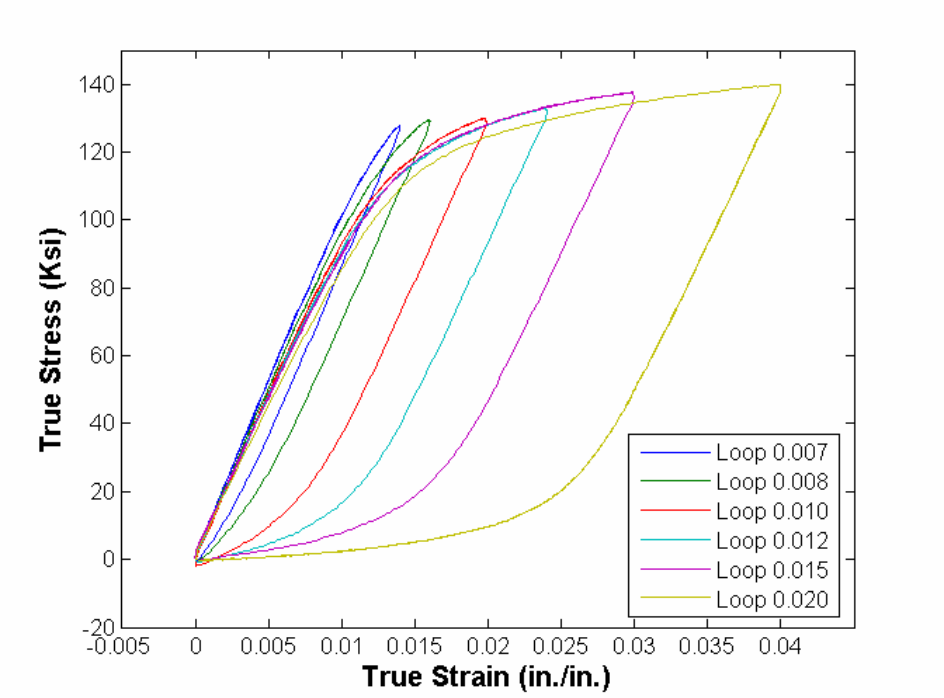

Figure B-8: UG3 Coupon Stabilized Hysteresis Loops With Compressive Peaks Shifted to Zero

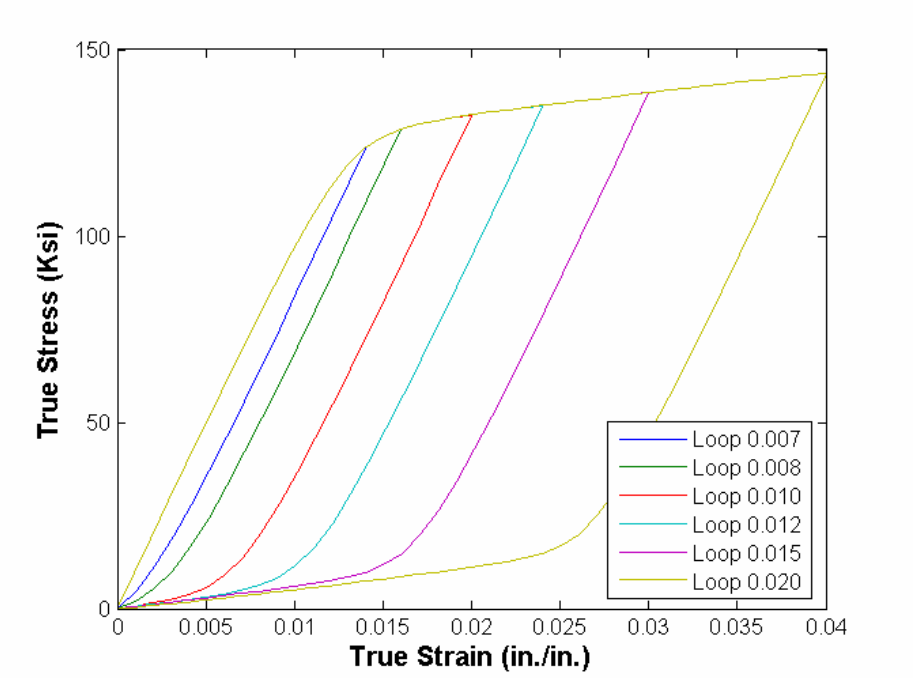

Figure B-9: Massing Hysteresis Loops With Compressive Peaks Shifted to Zero

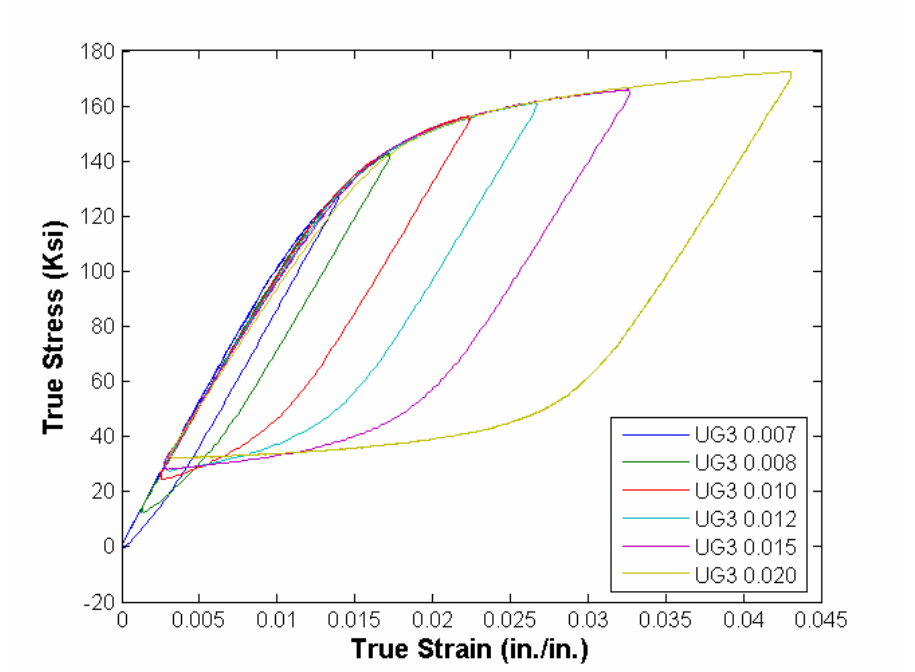

Figure B-10: UG3 Coupon Stabilized Hysteresis Loops With Compressive Peaks Shifted to Create Single Upper Branch Curve

THIS PAGE INTENTIONALLY LEFT BLANK

APPENDIX C
GRAIN ORIENTATION EFFECT PLOTS

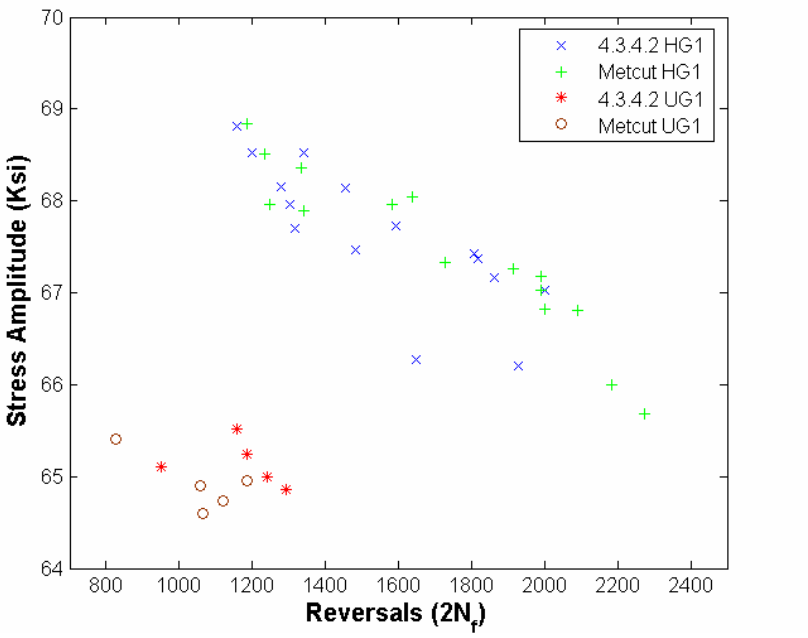

Figure C-1: Stress-Life Scatter of UG1 and HG1 Random Grain Orientation Coupons, 1.0% Strain Amplitude, 2.0% Load Drop Failure

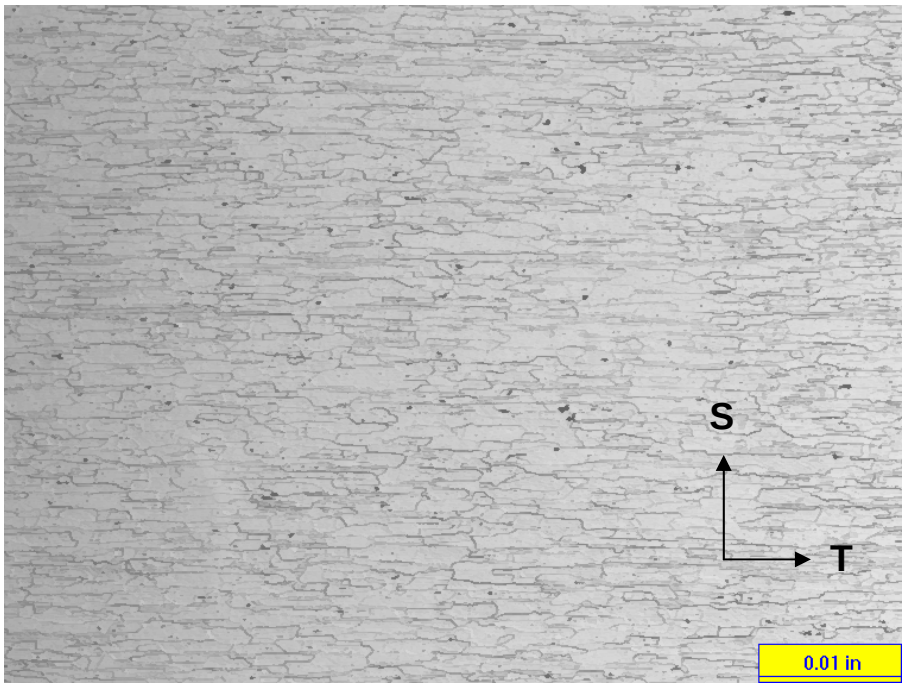

Figure C-2: Grain Orientation and Microtructure of Plate 1

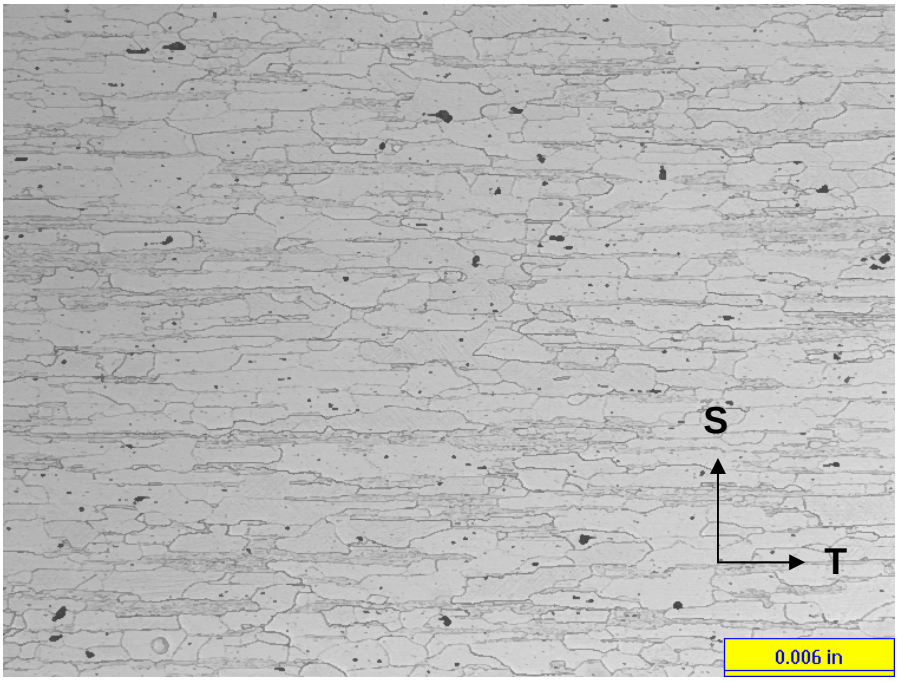

Figure C-3: Grain Orientation and Microtructure of Plate 1, Increased Magnification

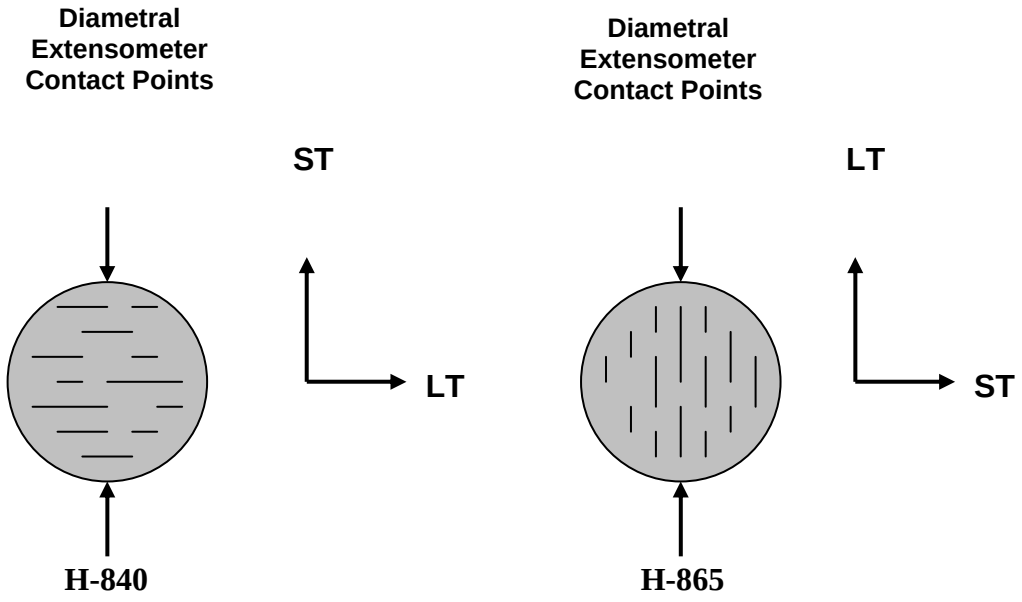

Figure C-4: Grain Orientation with Respect to Diametral Extensometer Placement for Two Hourglass Test Coupons

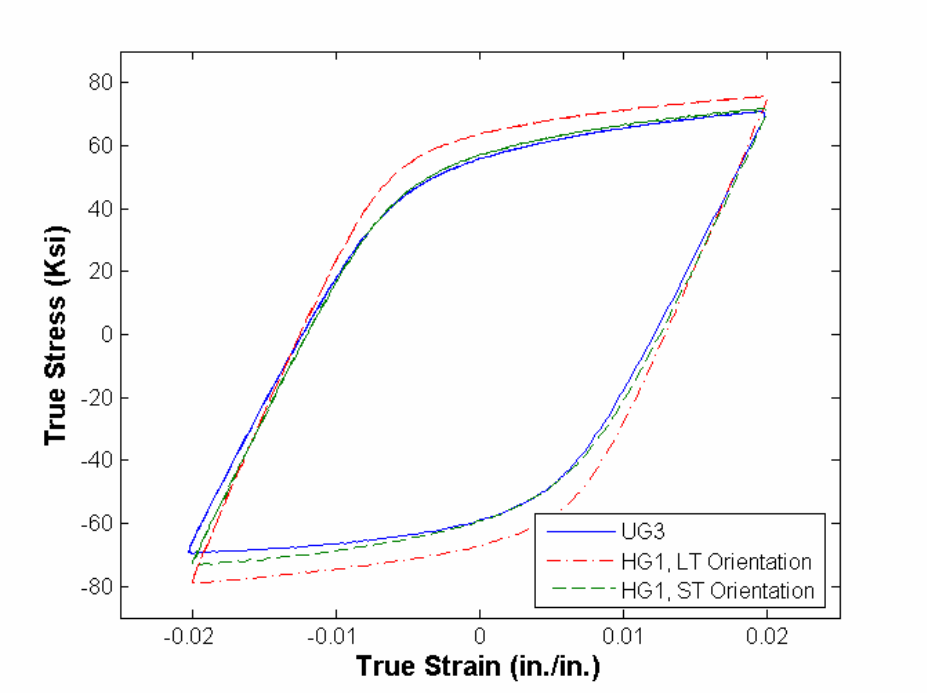

Figure C-5: Stabilized Hysteresis Loops for 2.0% Strain Amp., Uniform Gage and Hourglass Coupons

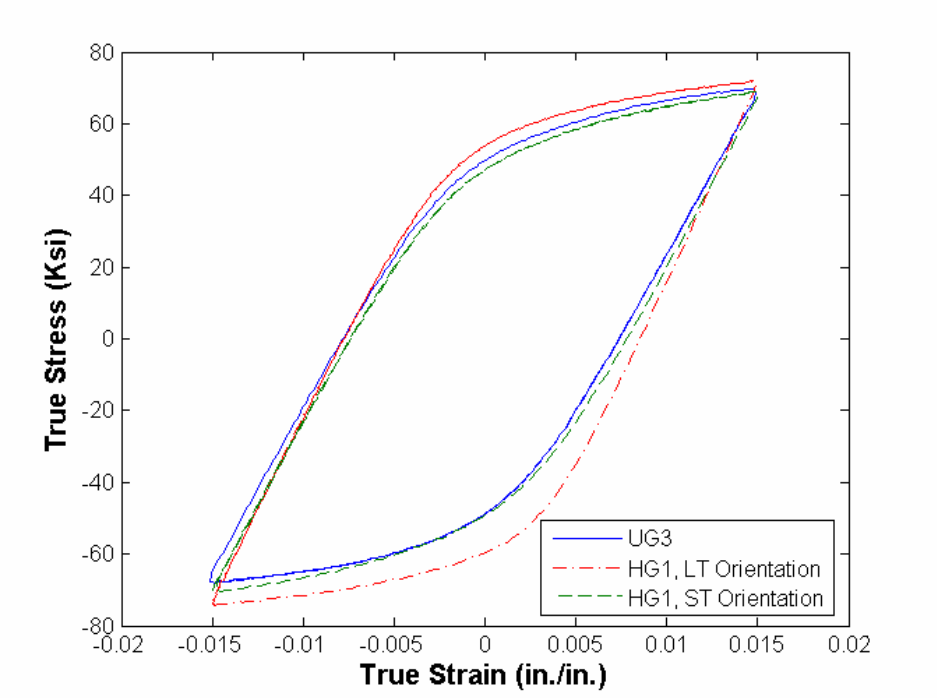

Figure C-6: Stabilized Hysteresis Loops for 1.5% Strain Amp., Uniform Gage and Hourglass Coupons

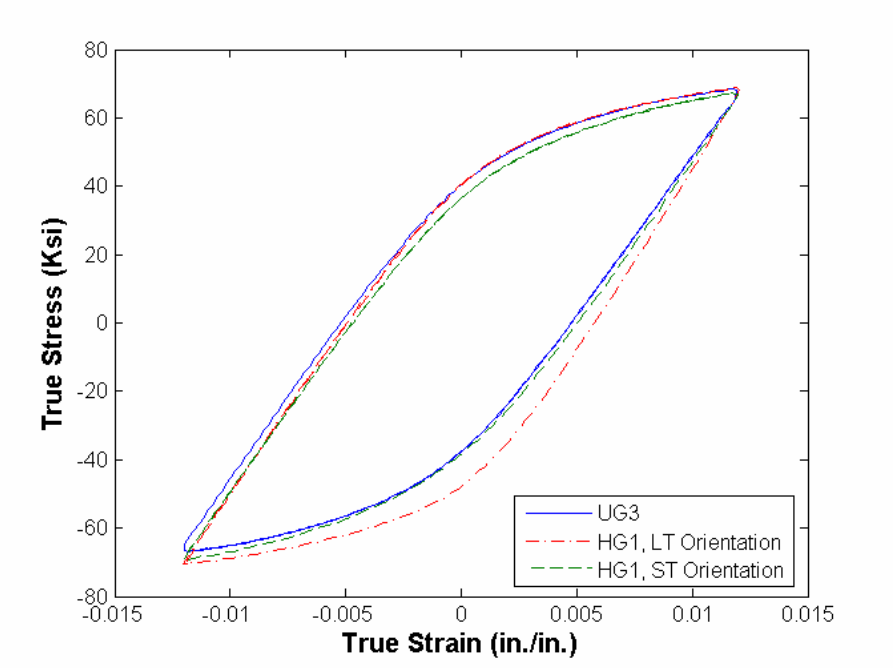

Figure C-7: Stabilized Hysteresis Loops for 1.2% Strain Amp., Uniform Gage and Hourglass Coupons

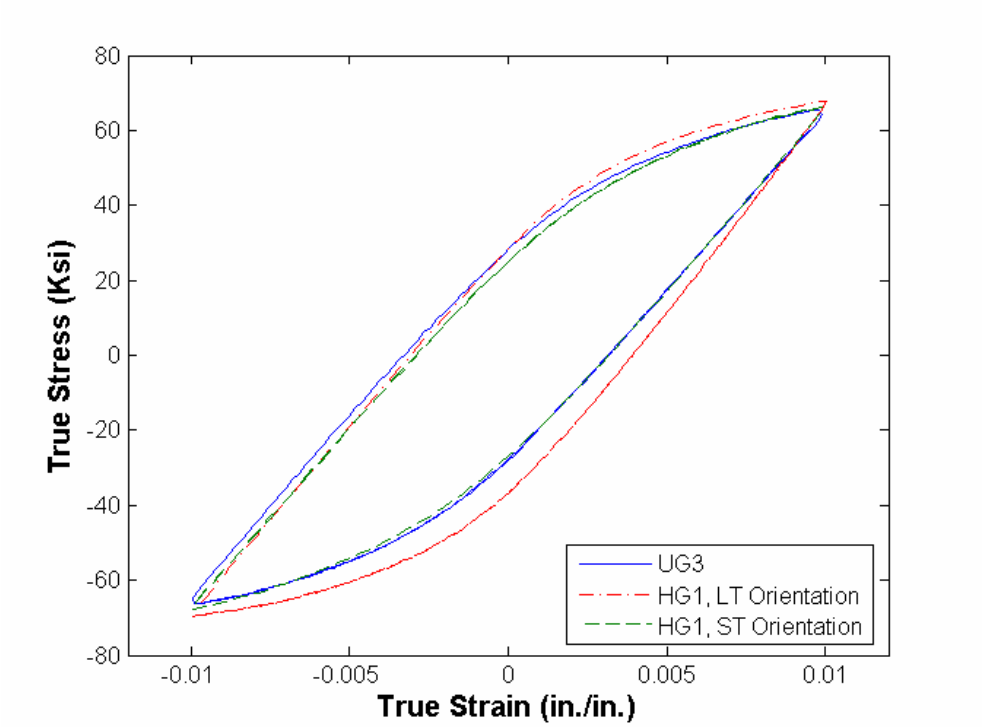

Figure C-8: Stabilized Hysteresis Loops for 1.0% Strain Amp., Uniform Gage and Hourglass Coupons

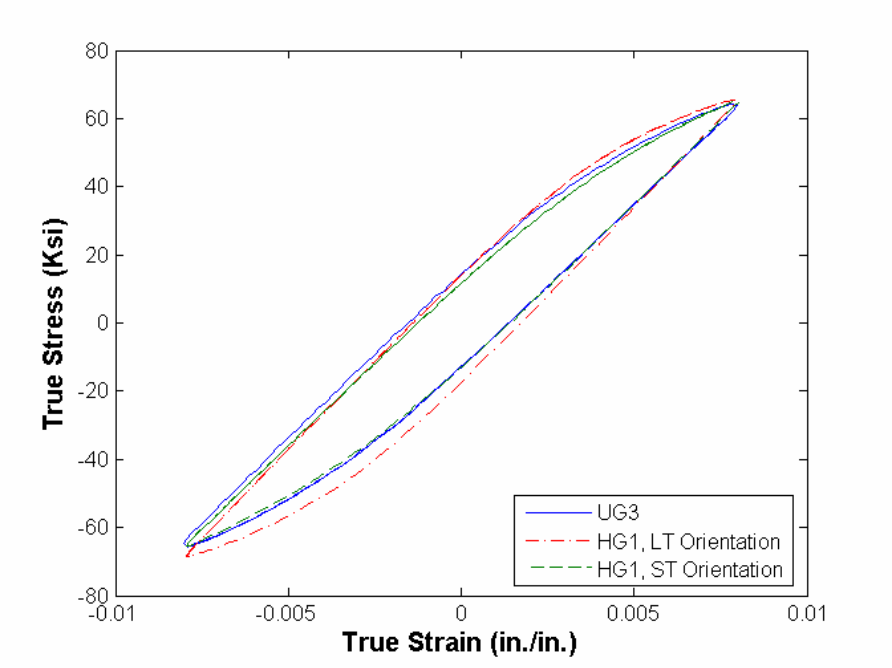

Figure C-9: Stabilized Hysteresis Loops for 0.8% Strain Amp., Uniform Gage and Hourglass Coupons

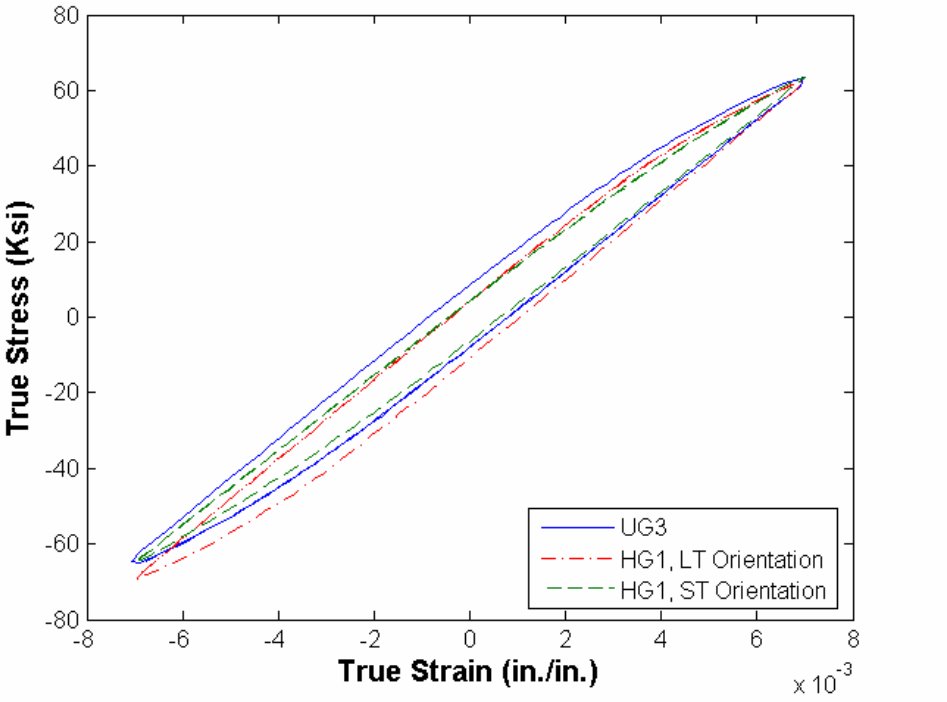

Figure C-10: Stabilized Hysteresis Loops for 0.7% Strain Amp., Uniform Gage and Hourglass Coupons

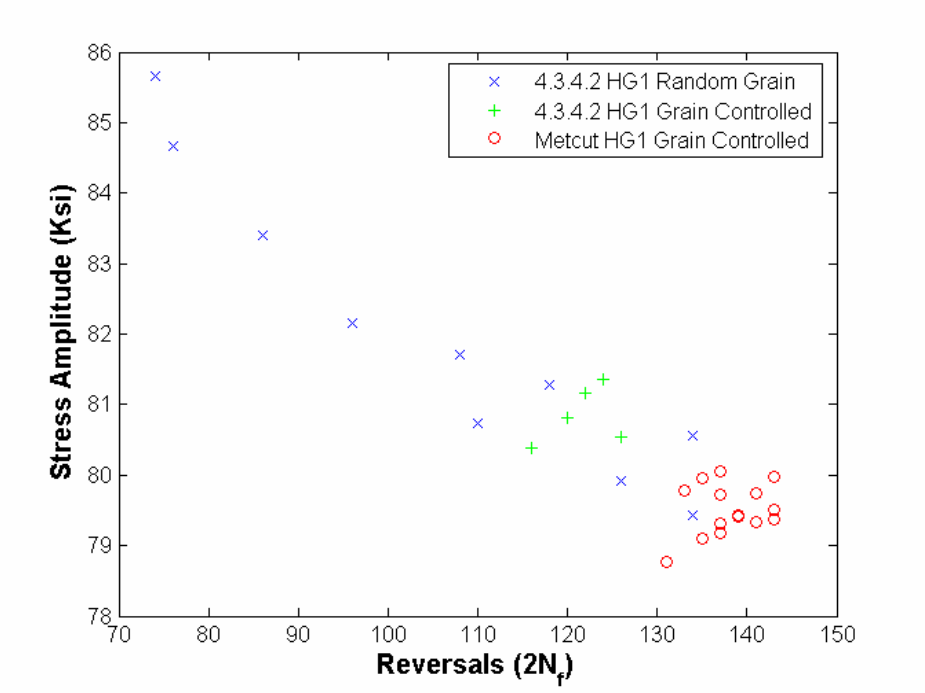

Figure C-11: Stress-Life Scatter of HG1 Random and Controlled Grain Orientation Coupons, 4.0% Strain Amplitude, 2.0% Load Drop Failure

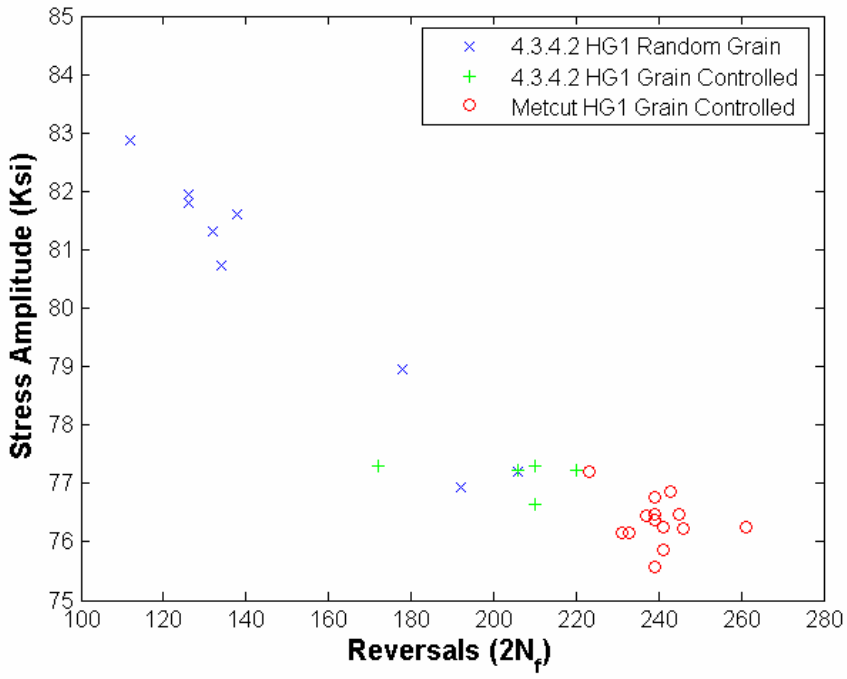

Figure C-12: Stress-Life Scatter of UG3 and HG1 Random and Controlled Grain Orientation Coupons, 3.0% Strain Amplitude, 2.0% Load Drop Failure

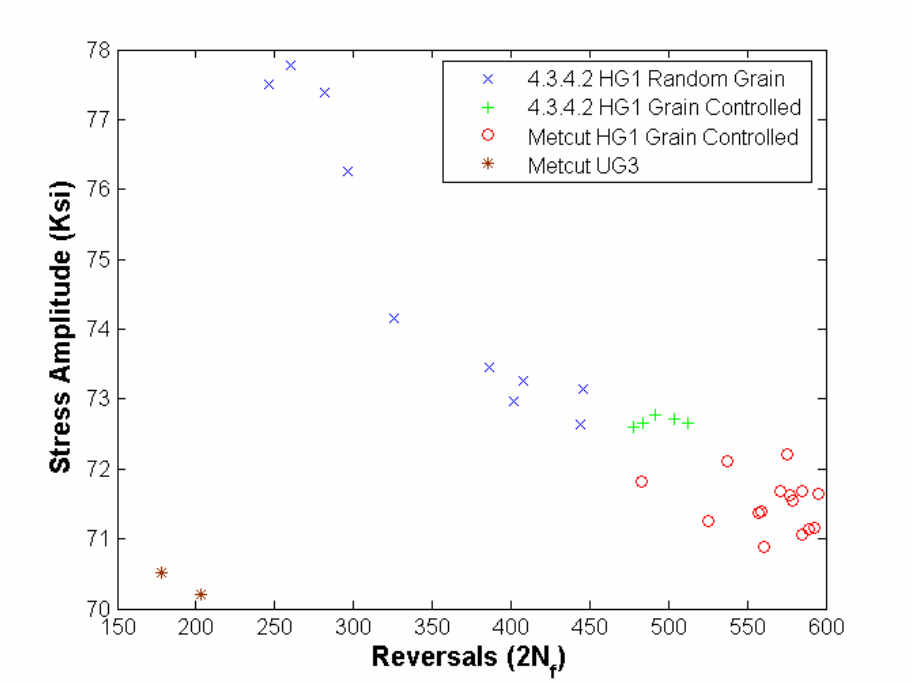

Figure C-13: Stress-Life Scatter of UG3 and HG1 Random and Controlled Grain Orientation Coupons, 2.0% Strain Amplitude, 2.0% Load Drop Failure

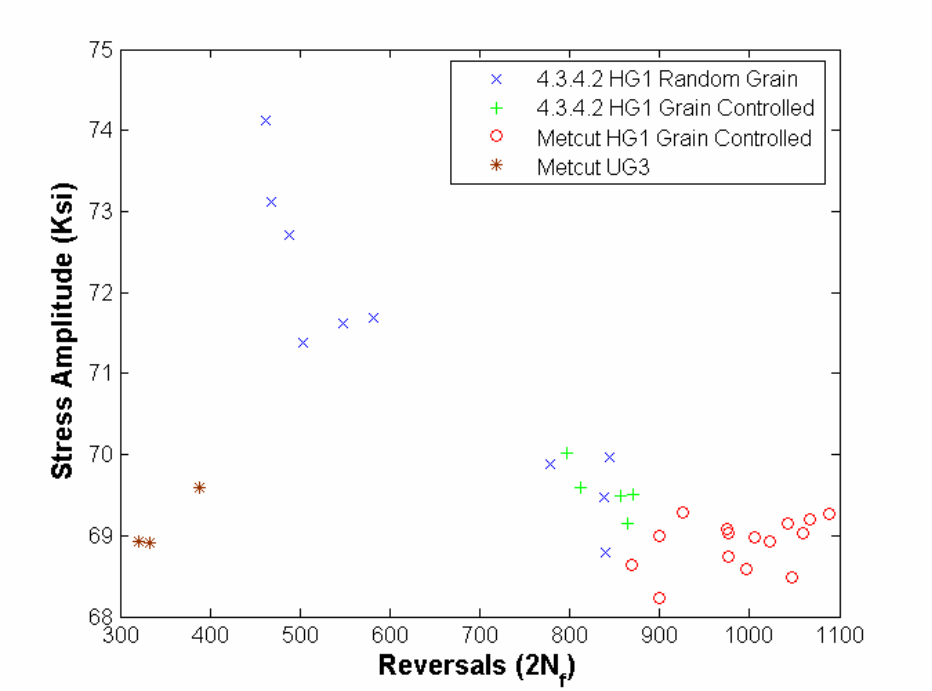

Figure C-14: Stress-Life Scatter of UG3 and HG1 Random and Controlled Grain Orientation Coupons, 1.5% Strain Amplitude, 2.0% Load Drop Failure

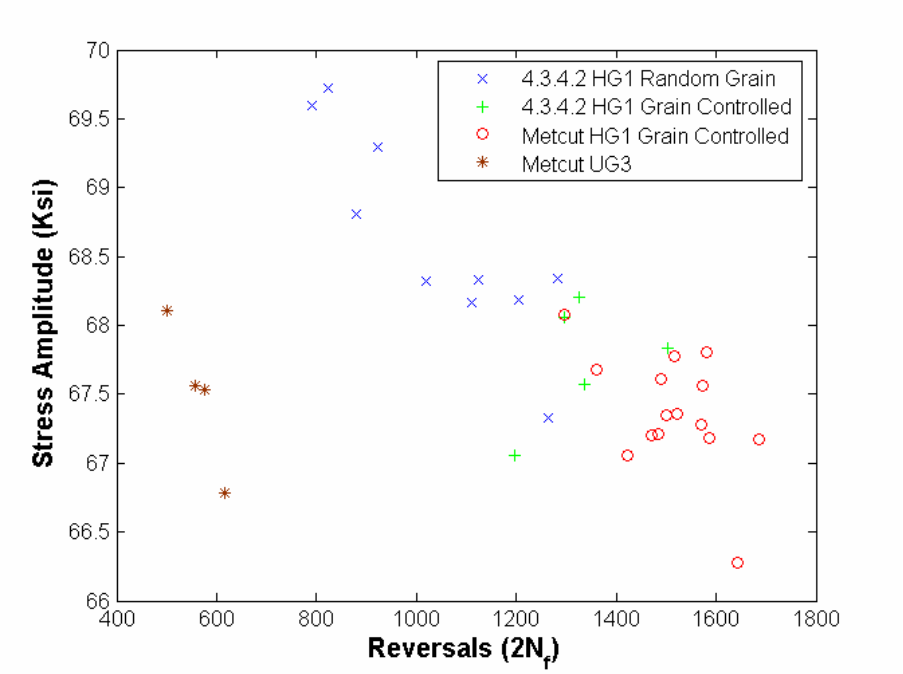

Figure C-15: Stress-Life Scatter of UG3 and HG1 Random and Controlled Grain Orientation Coupons, 1.2% Strain Amplitude, 2.0% Load Drop Failure

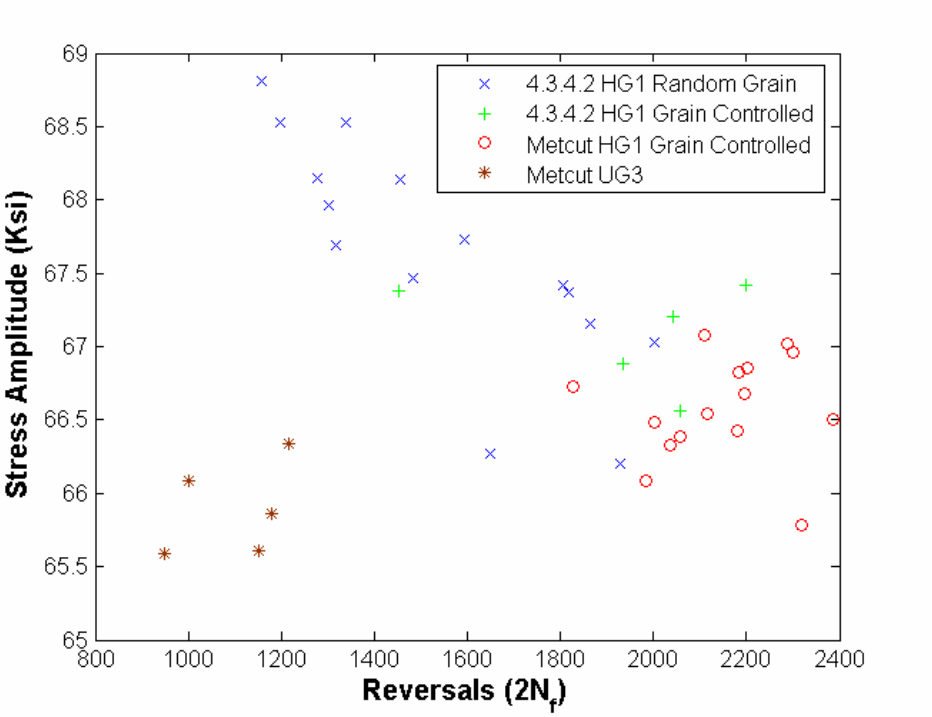

Figure C-16: Stress-Life Scatter of UG3 and HG1 Random and Controlled Grain Orientation Coupons, 1.0% Strain Amplitude, 2.0% Load Drop Failure

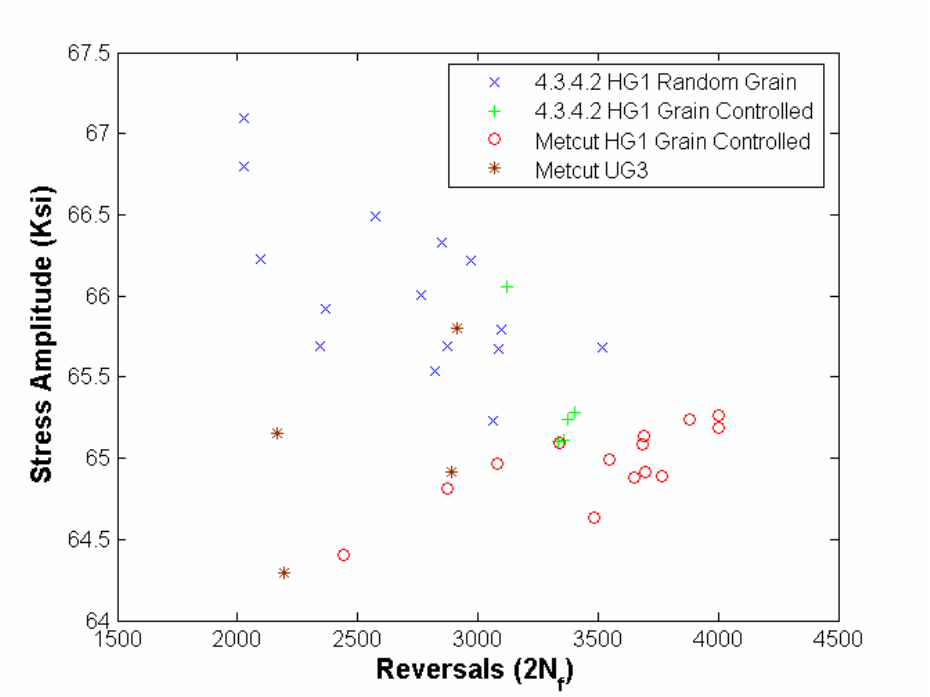

Figure C-17: Stress-Life Scatter of UG3 and HG1 Random and Controlled Grain Orientation Coupons, 0.8% Strain Amplitude, 2.0% Load Drop Failure

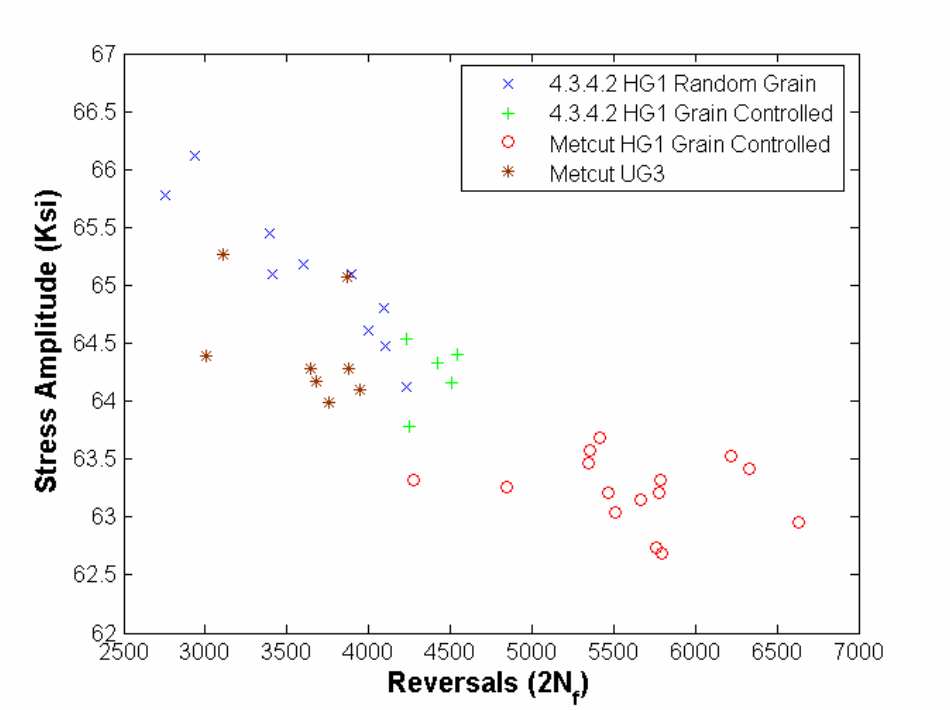

Figure C-18: Stress-Life Scatter of UG3 and HG1 Random and Controlled Grain Orientation Coupons, 0.7% Strain Amplitude, 2.0% Load Drop Failure

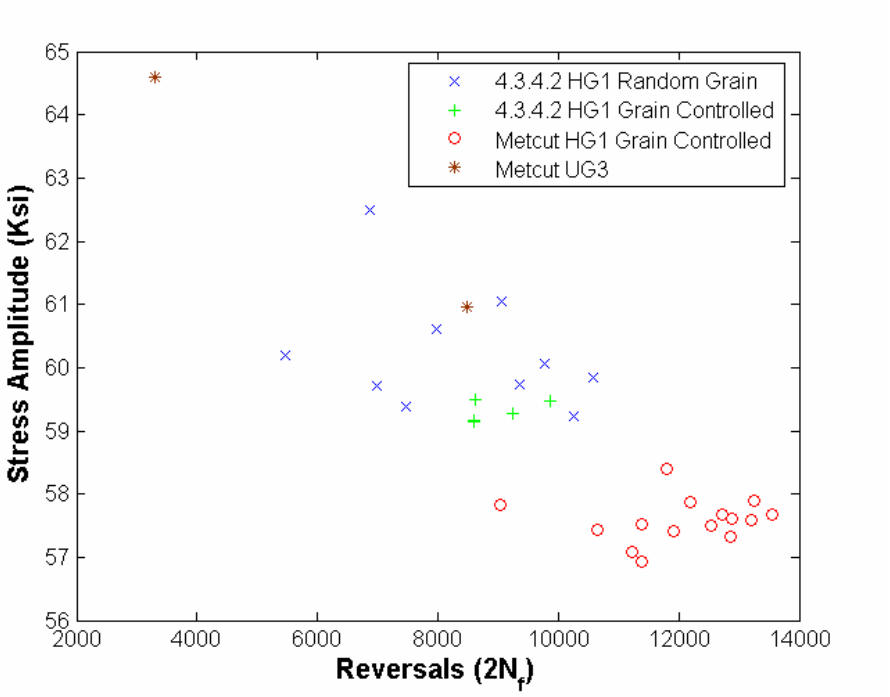

Figure C-19: Stress-Life Scatter of UG3 and HG1 Random and Controlled Grain Orientation Coupons, 0.6% Strain Amplitude, 2.0% Load Drop Failure

DISTRIBUTION:

NAVAIRSYSCOM (AIR-4.3.3), Bldg. 2187, Room 2340A (2)
48110 Shaw Road, Patuxent River, MD 20670
NAVAIRSYSCOM (AIR-5.1V), Bldg. 304, Room 120 (1)
22541 Millstone Road, Patuxent River, MD 20670-1606
NAVAIRSYSCOM (AIR-5.1), Bldg. 304, Room 100 (1)
22541 Millstone Road, Patuxent River, MD 20670-1606
NAVAIRWARCENACDIV (4.9.8.3), Bldg. 407, Room 116 (1)
22269 Cedar Point Road, Patuxent River, MD 20670-1120
NAVTESTWINGLANT (55TW01A), Bldg. 304, Room 200 (1)
22541 Millstone Road, Patuxent River, MD 20670-1606
DTIC (1)
8725 John J. Kingman Road, Suite 0944, Ft. Belvoir, VA 22060-6218